

# CHAPTER 4

---

## Briquetting and Pelletizing (Experimental-II)

The fourth chapter discusses the briquettes and pellets preparation and their testing. Taguchi technique was used, for selection of binder proportion in combination. To select the proper binder for pellets preparation, cylindrical shaped briquettes (diameter 9.75 mm and height 13-14 mm) were prepared and tested. Different binders like lime, slaked lime, bentonite, molasses etc. and their combination were used to prepare briquettes and their properties (compressive strength, drop strength and shatter index) were evaluated. From the results of briquettes' strength, pellets were prepared with combined binders (i.e. corn starch and molasses). Isothermal reduction in tubular furnace was carried out and weight loss method was used to find percentage of reduction. The activation energy was also calculated.

### 4.1 Briquette Preparation

#### 4.1.1 Stoichiometric Calculations:

The coal requirement for composite briquettes/pellets preparation with wastes are done as per stoichiometry calculation as follows.



$$(160) \quad (36) \quad (112)$$

Since, reduction of 160 g of  $\text{Fe}_2\text{O}_3$  requires 36 g of carbon

Therefore, reduction of  $W_{i0}$  g of  $\text{Fe}_2\text{O}_3$  requires  $(\frac{36}{160} \times W_{i0}) = 0.225W_{i0} = W_C$  g of carbon... (4.2)

where  $W_{i0}$  is the weight of  $\text{Fe}_2\text{O}_3$  present in waste,  $W_C$  is the weight of carbon required for reduction of  $\text{Fe}_2\text{O}_3$  in waste.

→ From proximate analysis of coal, fixed carbon content in coal =  $F_C$  pct

i.e.  $F_C$  g fixed carbon content in 100 g coal

Therefore, for  $W_C$  g carbon, coal required  $(\frac{100}{F_C} \times W_C) = W_{coal}$  g ... (4.3)

Where  $F_C$  pct fixed carbon content in coal,

$W_{coal}$  is the weight of coal required for reduction of  $\text{Fe}_2\text{O}_3$  present in waste.

Hence, Stoichiometric ratio  $(\frac{Fe_{tot}}{C}) = \frac{\text{Total Fe presence}}{\text{Carbon require}} = \frac{W_{i0} \times 0.7}{W_C}$  ... (4.4)

Details calculations of Coal Requirement is shown in Appendix 1.

**Table 4.1: Final pct of Fe<sub>2</sub>O<sub>3</sub> considering for pellet production**

<b>Assay →</b>	<b>Initial Fe<sub>(T)</sub>,pct (Raw material)</b>	<b>Final Fe<sub>(T)</sub>,pct (After beneficiation)</b>	<b>Final Fe<sub>2</sub>O<sub>3</sub>,pct</b>
JSW Dust	38.77	61.13	<b>87.33</b>
JSW Sludge	51.64	63.48	<b>90.69</b>
Vizag Sludge	49.49	60.04	<b>85.77</b>

#### **4.1.2 Binder Selection**

Binders play a very important role in the briquetting/pelletizing process. Binder is that material which serves as a bridge between the particles and thus increases the green or dry strength of the bonded particles. Functions of binders for iron ore palletization and requirements for selecting the binder are described in Section 2.5.

The role of the binders are as follows:

1. Improve the ball-formation of the material,
2. Affect the green and harden strength of pellets,
3. Adjust the chemical and mineralogical consistency, as well as quality of harden pellets.

#### **4.1.3 Briquette preparation**

To select the proper binder for pellets, initially cold bonded briquettes of waste-coal composite briquettes were prepared using a die and punch assembly by giving one impact to the moist powder mixture. The impact force was standardized by proper design of assembly. Diameter and height of the cylindrical shaped briquettes were 9.75 mm and 13 to 14 mm respectively. The weight of the briquettes varied between 2.0 to 2.20 g. After green briquettes formation that were exposed to CO<sub>2</sub> gas for 5 minutes (in some cases only) which favoured the formation of carbonate bonds between the particles. These briquettes were dried in open atmosphere for 24 hours.

The binder may be organic or inorganic materials. Initial trials for briquettes using various organic and inorganic binders were done only for JSW dust (as shown in Table 4.2); later, all the other wastes are also used for binder selection.

**Table 4.2: Raw materials used for composite briquettes**

Batch No.	JSW Dust, g	Coal, g	Addition of Coal	Fly Ash, g(pct)	Lime, g(pct)	Slake Lime, g(pct)	Molasses, g(pct)
TB1	500	158.45	As per stoichiometry	12.5(2.5)	25 (5)	--	25(5)
TB2	500	166.37	+ 5pct	25(5)	25(5)	--	25(5)
TB3	500	174.30	+10pct	37.5(7.5)	25(5)	--	25(5)
TB4	350	110.92	As per stoichiometry	35 (10)	--	17.5(5)	17.5(5)
TB5	300	99.82	+ 5pct	15(5)	--	15(5)	15(5)
TB6	300	104.58	+10pct	22.5 (7.5)	--	15(5)	15(5)

\*\* CO<sub>2</sub>gas was passed for 5 minutes after briquetting for all the above batches

#### 4.1.4 Testing of Briquettes

The properties of briquettes / pellets of interest are those properties which have bearing on its performance during handling and transportation until it is charged in the furnace, and subsequently on its behaviour inside the furnace. The success of the cold bonding process depends heavily on attaining sufficient strength of the composite pellets. Some of the room temperature physical and mechanical properties have been tested and results are reported in this section.

##### 4.1.4.1 Drop test:

In the drop test, the briquettes or pellets were dropped repeatedly from a height of 0.457 m on a 10 mm thick steel plate until they break. The number of drops, before breaking of the briquette / pellet, was counted and noted down. The final value was taken as the average of three/four such test values. These drop tests were done for green as well as dried briquette / pellet.

#### 4.1.4.2 Compression test:

This test was performed by applying uniaxial compressive load at a constant rate and compressive strength was taken as the force required to break the briquette / pellet. Each briquette / pellet was squeezed between two plates under increased applied load. The value of the load at which the briquette/ pellet developed crack/break was recorded as strength of the briquette / pellet. The final value was calculated as the arithmetic mean of four such test values. The compressive strengths of the briquettes / pellets were measured on tensometer (Make: Mikrotech, Pune).

#### 4.1.4.3 Shatter test:

The known amounts of briquettes / pellets were dropped from a standard height of 2 m on a 10 mm thick steel plate for 4 times. The broken sample pieces were put on a 100 mesh sieve. The amount of the material passed through the sieve, with respect to the original weight, was indicated as the shatter index.

$$\text{Shatter index (pct)} = \frac{\text{Weight of } -100 \text{ mesh fraction}}{\text{Initial weight of sample}} \times 100 \quad \dots(4.5)$$

#### 4.1.5 Testing Results of Briquettes

**Table 4.3:Results of drop test for composite briquette of JSW dust**

Batch No.	Green Drop Test				Dry Drop Test				Remarks
	S1	S2	S3	Avg	S1	S2	S3	Avg	
	TB1	2	3	3	<b>3</b>	-	-	-	
TB2	3	4	4	<b>4</b>	8	8	10	<b>8</b>	Compare to batch TB1, good green and dry drop results
TB3	8	8	7	<b>8</b>	22	24	26	<b>24</b>	Excellent dry drop result among all batches
TB4	7	6	6	<b>6</b>	9	8	9	<b>9</b>	Comparatively moderate dry and green drop result
TB5	6	6	5	<b>6</b>	8	9	8	<b>8</b>	Comparatively moderate dry and green drop result
TB6	8	6	5	<b>6</b>	11	9	10	<b>10</b>	Comparatively moderate dry and green drop result

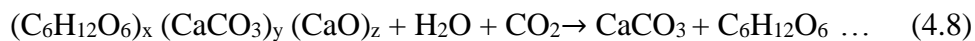
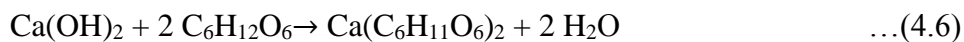
**Table 4.4: Results of compression and shatter tests for composite briquette of JSW dust**

Batch No.	Compressive Strength (N/Briquette)				Shatter Index (pct)	Remarks
	S1	S2	S3	Avg		
TB1	-	-	-	-	-	After drying pellets breaks, so test was not done.
TB2	49	58.8	49	52.27	22.59	Comparatively low compressive strength and higher shatter index → Poor results
TB3	98	107.8	88.2	98.0	9.84	Comparatively good compressive strength and better shatter index
TB4	88.2	98	88.2	91.47	16.23	Comparatively good compressive strength and higher shatter index
TB5	68.6	68.6	49	62.07	5.53	Comparatively low compressive strength and Excellent shatter index
TB6	127.4	107.8	88.2	107.8	7.17	Comparatively higher compressive strength and good shatter index

The binder trial runs for JSW dust was tested as per standard procedure and the results are presented in Tables 4.3 and 4.4.

It was found that TB3 (with 7.5 pct fly ash, 5 pct lime and 5 pct molasses) gave good green and dry strength, but TB6 (with 7.5 pct fly ash, 5 pct slake lime and 5 pct molasses) gave higher compressive strength and as well as good shatter strength; that means slake lime was more effective to form calcite due to CO<sub>2</sub> passing.

The calcite forming reaction, with the catalytic action of glucose can be expressed as follows[74]:



Further trials were done with starch and molasses as binder separately with JSW dust and the results were tabulated (Table 4.6). The starch was formed from corn powder. Starch is a carbohydrate. It does not dissolve in cold water and decomposes very easily. The starch has other advantages as binder, such as easy burn out, environment friendly and inexpensive. After careful analysis it was observed the results were promising with starch and molasses when the

percentage of binder was more than 5 pct. The combination of binder (starch and molasses) were then tested using design of experiments.

Further trials were done with two different organic binders in varying percentage (Table 4.5) and the test results are presented in Table 4.6. The data represents for the experiment runs are the average of three samples. It was found that 10 pct starch or 10 pct molasses giving very good results without CO<sub>2</sub> gas passed.

**Table 4.5: Different amount of binders used for briquettes**

Sr.No.	Binder Composition	Coal
1.	5pct Starch	As per Stoichiometric calculations
2.	10pct Starch	
3.	10pct Molasses	

**Table 4.6: Results of briquettes using starch or molasses**

Batch No.	Binder used	No. of Stroke	Drop No.	Shatter Index (pct)	Strength (N/Briquette) (Average)
TB7	5pct Starch	3 strokes	11	22.01	78.4
TB8	10pct Starch	3 strokes	>150	0.52	431.2
TB9	10pct Molasses	3 strokes	>150	0.31	833.0

**\*\* CO<sub>2</sub> gas did not passed after briquetting**

## **4.2 Design of Experiments**

Experimental work for the briquetting is carried out in such a way that minimum number of experiments can give output as desired. For this *design of experiment* methodology is applied to select the runs of experiment. After the selection of *orthogonal array* and experiment combinations, Taguchi technique was used with two variable (starch and molasses) and three levels (2.5pct, 5.0 pct and 7.5pct of each).

The design of experiments (DOE) is the design of any task that aims to describe or explain the variation of information under conditions that are hypothesized to reflect the variation. The term is generally associated with true experiments in which the design introduces conditions that directly affect the variation but may also refer to the design of quasi-experiments, in which natural conditions that influence the variation are selected for observation.

### **4.2.1 Taguchi Method**

The Taguchi method was developed by Genichi Taguchi, Japan. Taguchi method has been widely utilized in engineering analysis and consist of a plan of experiments with the objective of acquiring data in a controlled way, in order to obtain information about the behavior of a given process[110].The Taguchi design involves orthogonal arrays to organize the parameters affecting particular property of interest and the levels at which they vary. It allows the selection of the necessary data to determine the factors affecting product quality the most with a minimum number of experiments. So, it saves time and resources.Tosum and Ozler[111] used the Taguchi method to investigate multiple performance characteristics and the improvement of optimal cutting parameters in hot turning operations. Srinivas and Venkatesh[112] proposed the efficient use Taguchi's parameter design to obtain optimum condition because it leads to minimum number by experimental and lower cost. Ross[113] reviewed the optimization method of the manufacturing parameters using Taguchi method. He observed that the experiment design of the orthogonal array of the Taguchi method could identify the significant foaming parameters to adjust the process.

#### **4.2.2 Steps for Taguchi Method[114]**

1. Problem identification,
2. Brainstorming (identifying factors, factor levels, possible interactions, objectives),
3. Experimental design (choosing orthogonal arrays, and designing of experiments),
4. Run of the experiments and analyze the results,
5. Confirmation (i.e. reproducibility) runs.

#### **4.2.3 Selection of Parameters and Levels**

It was identified by fish bone diagram(Figure 4.1), the process parameters which will influence strength and shatter index of the briquettes. Use of one organic binder was not giving good results. Combination of organic binders were used, aiming for better results. The binders along with their levels are shown in Table4.7.

#### **4.2.4 Selection of Orthogonal Array**

After identification of the problem, factors contributing could be found out with the help of cause and effect diagram. Dhole et al[115]was used the similar approach of pointing the affecting parameters out by formulating cause and effect diagram(Figure 4.1). Cause-effect diagram was generally used for the selection of affecting parameters on the property of interest. In this study two properties of interest are: strength and shatter index. But eventually both properties are getting affected by the similar factors. Figure 4.1 shows the cause-effect diagram for the briquette strength and shatter index as properties of interest and all branches shows the factors affecting briquette strength and shatter index.

**Cause and Effect Diagram for Pellet Strength and Shatter Index**

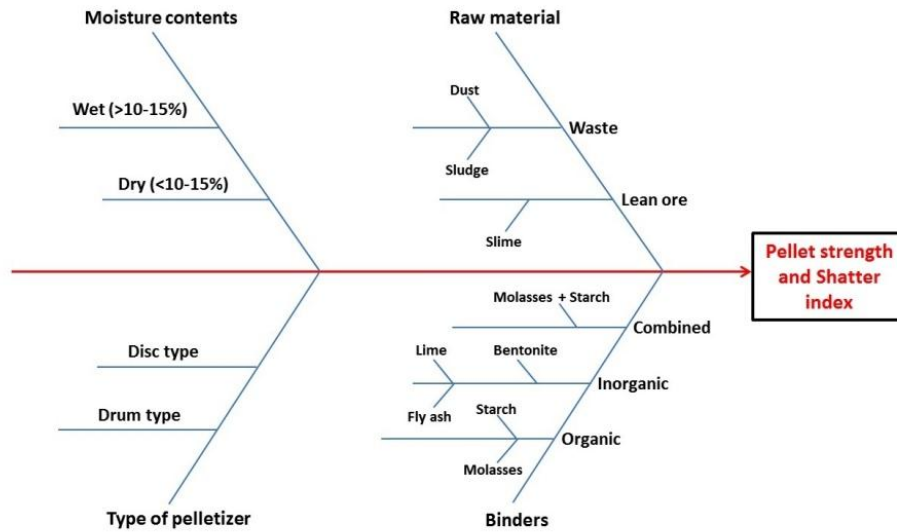


**Fig. 4.1: Cause-effect diagram for the pellet strength and shatter index**

Further design matrix needs to be constructed depending upon the number of factors and levels of them. This specially designed matrix is called orthogonal array (OA). Commonly used OA includes one of the L4, L9, L12, L18, and L27 arrays. The columns in the OA indicates the factor and its corresponding levels, and each row in the OA constitutes an experimental run which is performed at the given factor combination and their current levels.

Typically, either 2 or 3 levels were chosen for each factor. There were two different organic binders used and each had three different levels. So, total nine experiments could be performed including all possibilities to check the effect of different combinations on the properties of interest i.e. briquette strength and shatter index. All the experiments were performed as such they were only nine. Using standard catalogue of Taguchi orthogonal array in software Minitab 15 was used the L9 orthogonal array for the experimentations as shown in Table 4.8.

The results of the L9 orthogonal array is presented in Table 4.9 in terms of strength and shatter index as output parameter, which tested and average of three values are finalized.

**Table4.7: Selected parameters and their levels for 2X3 for JSW dust**

<b>Parameters</b>	<b>Level-1</b>	<b>Level-2</b>	<b>Level-3</b>
Binder-S (Starch)	2.5pct	5.0 pct	7.5pct
Binder-M (Molasses)	2.5pct	5.0 pct	7.5pct

**\*\* CO<sub>2</sub>gas did not passed after briquetting**

**Table4.8: L9 orthogonal array for 2X3 for JSW dust**

<b>Experiment Run</b>	<b>Starch Levels, pct</b>	<b>Molasses Levels, pct</b>
E1	2.5	2.5
E2	2.5	5.0
E3	2.5	7.5
E4	5.0	2.5
E5	5.0	5.0
E6	5.0	7.5
E7	7.5	2.5
E8	7.5	5.0
E9	7.5	7.5

**Table 4.9: Experimental results for 2X3 JSW dust**

<b>Experiment Run</b>	<b>Starch Levels, pct</b>	<b>Molasses Levels, pct</b>	<b>Strength (N/briquette)</b>	<b>Shatter Index (pct)</b>
E1	2.5	2.5	451.26	0.84
E2	2.5	5.0	1196.82	0.18
E3	2.5	7.5	853.47	0.4
E4	5.0	2.5	794.61	0.53
E5	5.0	5.0	1059.48	0.84
E6	5.0	7.5	784.8	0.86
E7	7.5	2.5	1010.43	0.87
E8	7.5	5.0	1167.39	0.4
E9	7.5	7.5	873.09	0.35

**Table 4.10: Ranking order considering strength as priority**

<b>Rank</b>	<b>Experiment Run</b>	<b>Starch Levels, pct</b>	<b>Molasses Levels, pct</b>	<b>Strength (N/briquette)</b>	<b>Shatter Index (pct)</b>
1	E2	2.5	5.0	1196.82	0.18
2	E8	7.5	5.0	1167.39	0.40
3	E5	5.0	5.0	1059.48	0.84
4	E7	7.5	2.5	1010.43	0.87
5	E9	7.5	7.5	873.09	0.35
6	E3	2.5	7.5	853.47	0.40
7	E4	5.0	2.5	794.61	0.53
8	E6	5.0	7.5	784.8	0.86
9	E1	2.5	2.5	451.26	0.84

The ranking of the experiments was done by weighted and average method for both the output

parameter individually and the considering them simultaneously. The results are presented in Tables 4.10 to 4.12. It was found that E2 (with 2.5 pct starch and 5.0 pct molasses) gave highest strength and lower shatter index.

**Table 4.11: Ranking order considering shatter index as priority**

Rank	Experiment Run	Starch levels, pct	Molasses levels, pct	Strength (N/briquette)	Shatter Index (pct)
1	E2	2.5	5.0	1196.82	0.18
2	E9	7.5	7.5	873.09	0.35
3	E8	7.5	5.0	1167.39	0.4
4	E3	2.5	7.5	853.47	0.4
5	E4	5.0	2.5	794.61	0.53
6	E5	5.0	5.0	1059.48	0.84
7	E1	2.5	2.5	451.26	0.84
8	E6	5.0	7.5	784.8	0.86
9	E7	7.5	2.5	1010.43	0.87

Since both the properties are equally important, for considering combined effect of both, the sum of the ratio-1 and ratio-2 was considered and compared with each other for rankings.

$$\text{Ratio - 1} = \frac{\text{strength reading for particular exp.run}}{\text{maximum strength reading}} \quad (\text{always} \leq 1)$$

...(4.9)

$$\text{Ratio - 2} = \frac{\text{minimum shatter index reading}}{\text{shatter index reading for particular exp.run}} \quad (\text{always} \leq 1)$$

...(4.10)

**Table 4.12: Ranking order considering effect of both outputs**

Rank	Experiment Run	Starch levels, pct	Molasses levels, pct	Strength (N/briquette)	Shatter Index(pct)
1	E2	2.5	5.0	1196.82	0.18
2	E8	7.5	5.0	1167.39	0.4
3	E9	7.5	7.5	873.09	0.35
4	E3	2.5	7.5	853.47	0.4
5	E5	5.0	5.0	1059.48	0.84
6	E7	7.5	2.5	1010.43	0.87
7	E4	5.0	2.5	794.61	0.53
8	E6	5.0	7.5	784.8	0.86
9	E1	2.5	2.5	451.26	0.84

Minitab 15 statistical software was used for the analysis of the results. This software is a trusted software worldwide. The G. H. Patel College of Engineering and Technology, Gujarat is having a license version of this software. The graphs generated by the software includes individual and interaction plots of data means as well as individual and interaction plots of Signal (S) to Noise (N) ratio for strength and shatter index.

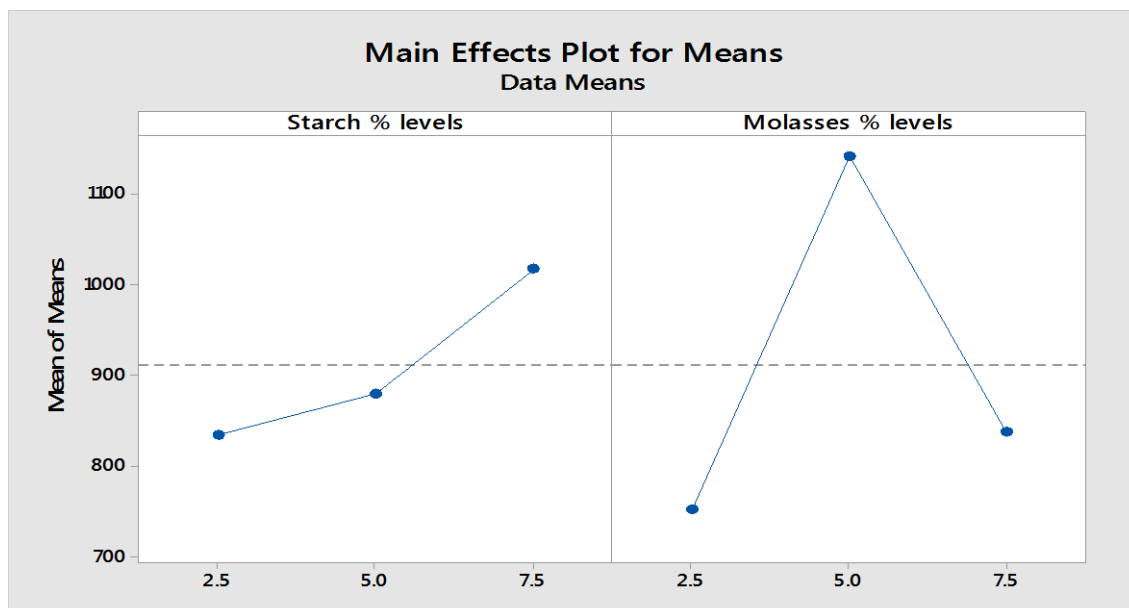


**Fig 4.2: Individual plot for briquette strength**

The grand mean or mean of means is the mean of the means of several subsamples, as long as the subsamples have the same number of data points. For example, consider several lots, each containing several items. The items from each lot are sampled for a measure of some variable and the means of the measurements from each lot are computed. The mean of the measures from each lot constitutes the subsample mean. The mean of these subsample means is then the grand mean.

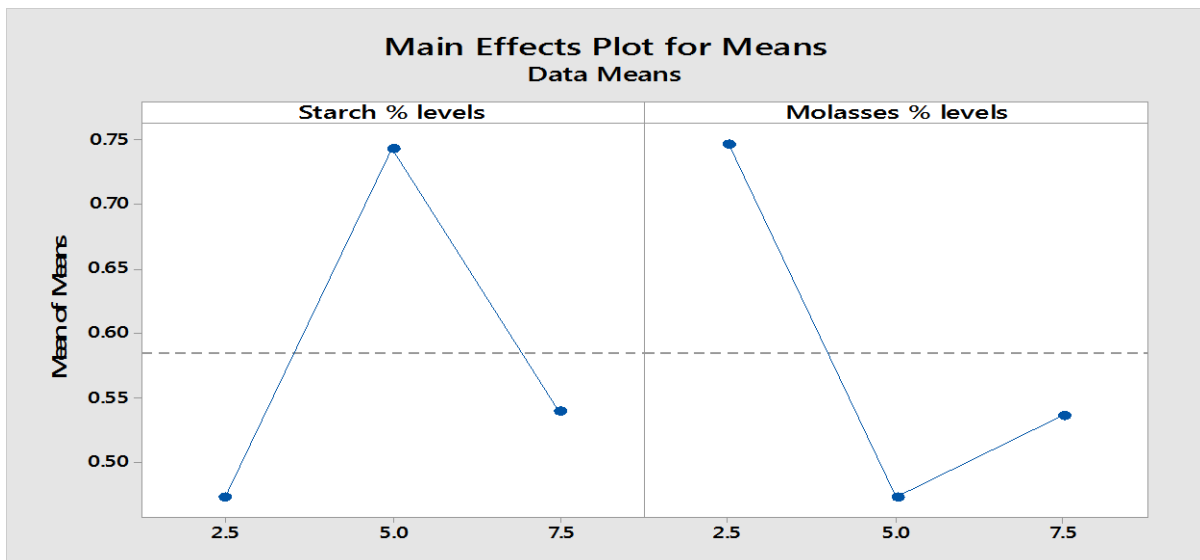


**Fig 4.3: Individual plot for shatter index**

From Figure 4.2 it was found that the strength, increased with increasing percentage of starch while for molasses gave peak at 5pct and then falls. On the other hand, in Figure 4.3 showed for shatter index, increasing starch percentage gave peak at 5pct and then decreases while increasing in molasses percentage gave the minimum value at 5pct.

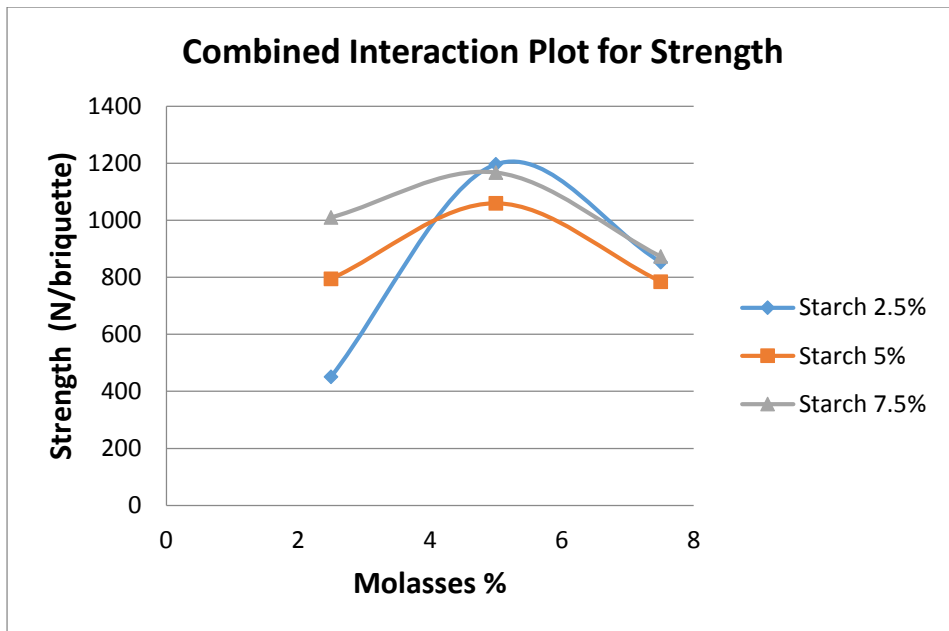


**Fig. 4.4(a): Interaction plot for briquette strength due to molasses**

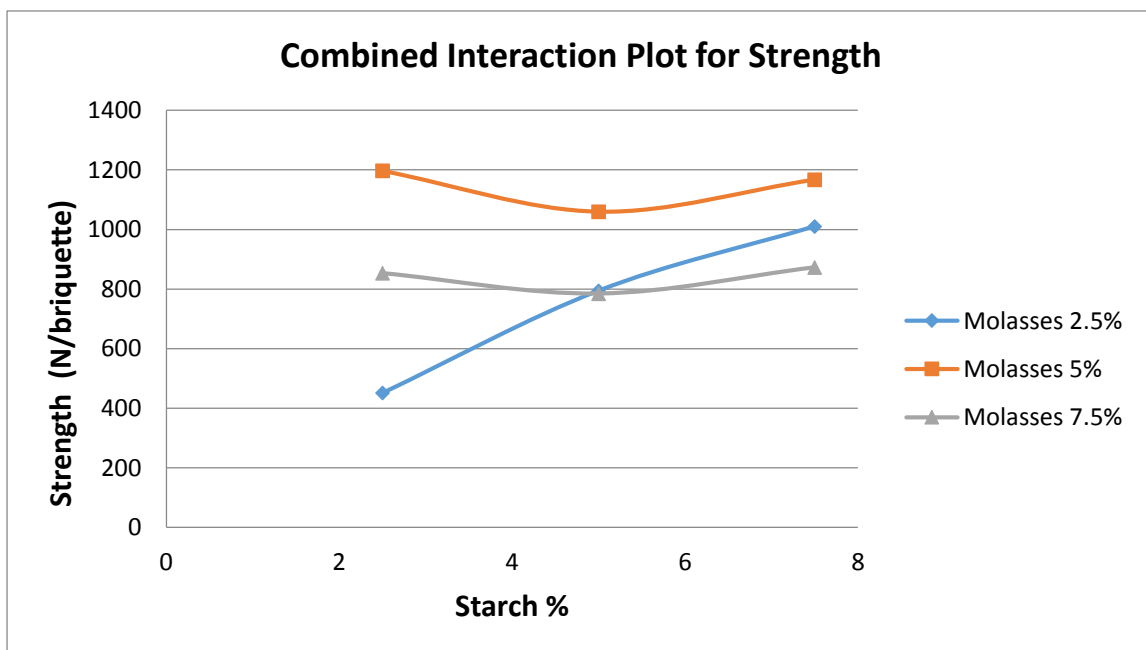


**Fig. 4.4 (b): Interaction plot for briquette strength due to starch**

Figure 4.4 shows all the nine strength readings for different combinations of the binder percentage. It indicated that the highest pellet strength was obtained with 5pct molasses + 2.5pct starch. Also, 5pct molasses individually gave higher strengths irrespective of starch percentage. Similarly, 7.5pct starch individually gave higher strengths as well.

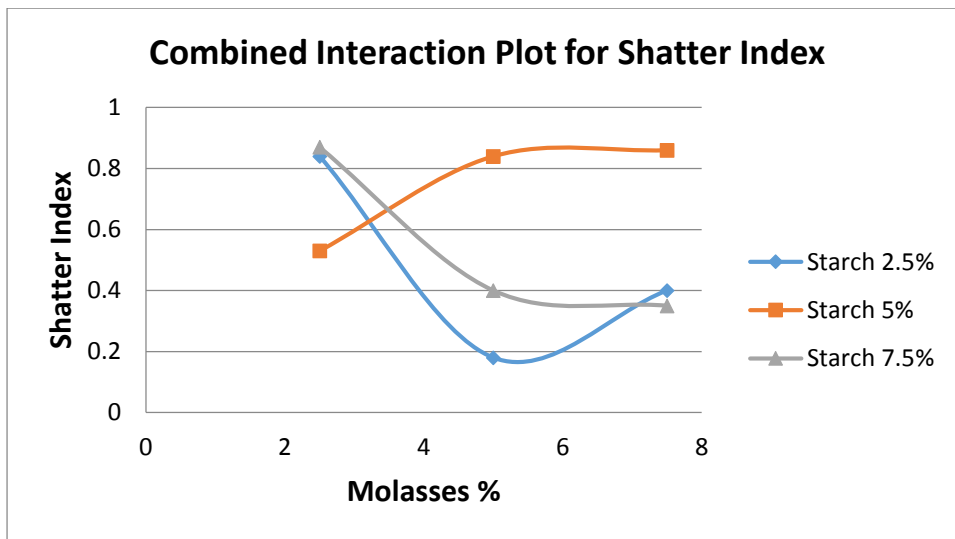


**Fig. 4.5 (a): Interaction plot for shatter index due to molasses**

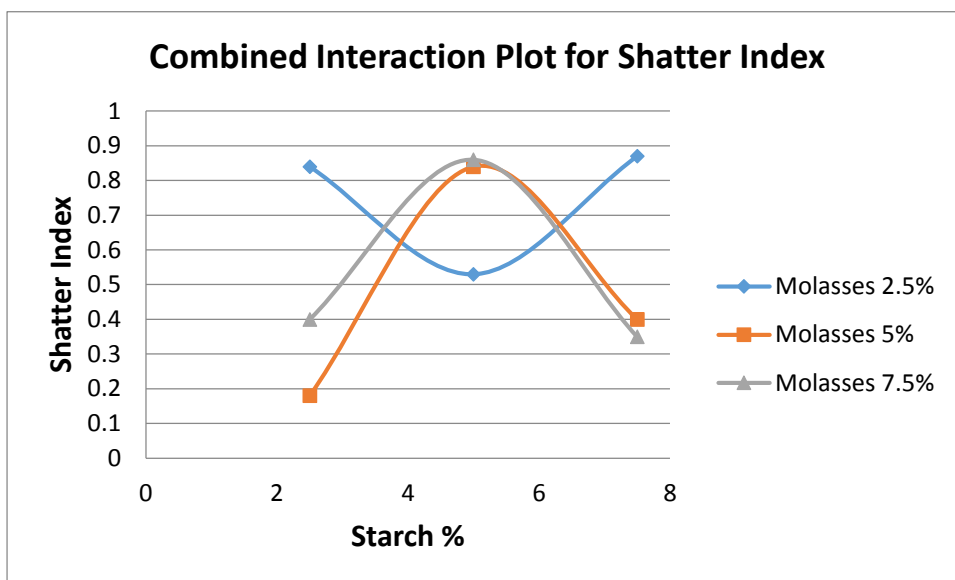


**Fig. 4.5 (b): Interaction plot for shatter index due to starch**

Figure 4.5 shows all the nine readings of shatter index for different combinations of the binder percentage. It indicated that the lowest shatter index was obtained with combination of 5pctmolasses and 2.5pctstarch. Also, 5pctmolasses individually gave lower shatter index irrespective of starch percentage. Similarly, 2.5pctstarch individually gave lower shatter index as well.

In Taguchi's design method of the design parameters (factors that can be controlled by designers) and noise factors (factors that cannot be controlled by designers, such as environmental factors) are considered influential on the properties. The signal (S) to noise (N)

ratio [(S/N)] is used in this analysis which takes both the mean and the unaccounted variability of the experimental result into account. The (S/N) ratio depends on the quality characteristics of the product/process to be optimized. The (S/N) ratio values will lead to rank the combination of binders and finally to get the optimum one.

Equation for signal to noise(S/N) ratio for characteristics lower is better can be given as follows:

$$\left(\frac{S}{N}\right)_{LB} = -10 \log \left[ \frac{1}{r} \sum_{i=1}^r y_i^2 \right] \quad \dots(4.11)$$

Equation for signal to noise(S/N) ratio for characteristics higher is better can be given as follows:

$$\left(\frac{S}{N}\right)_{HB} = -10 \log \left[ \frac{1}{r} \sum_{i=1}^r \frac{1}{y_i^2} \right] \quad \dots(4.12)$$

where  $y_i$  = Mean of data

r = No. of measured parameter

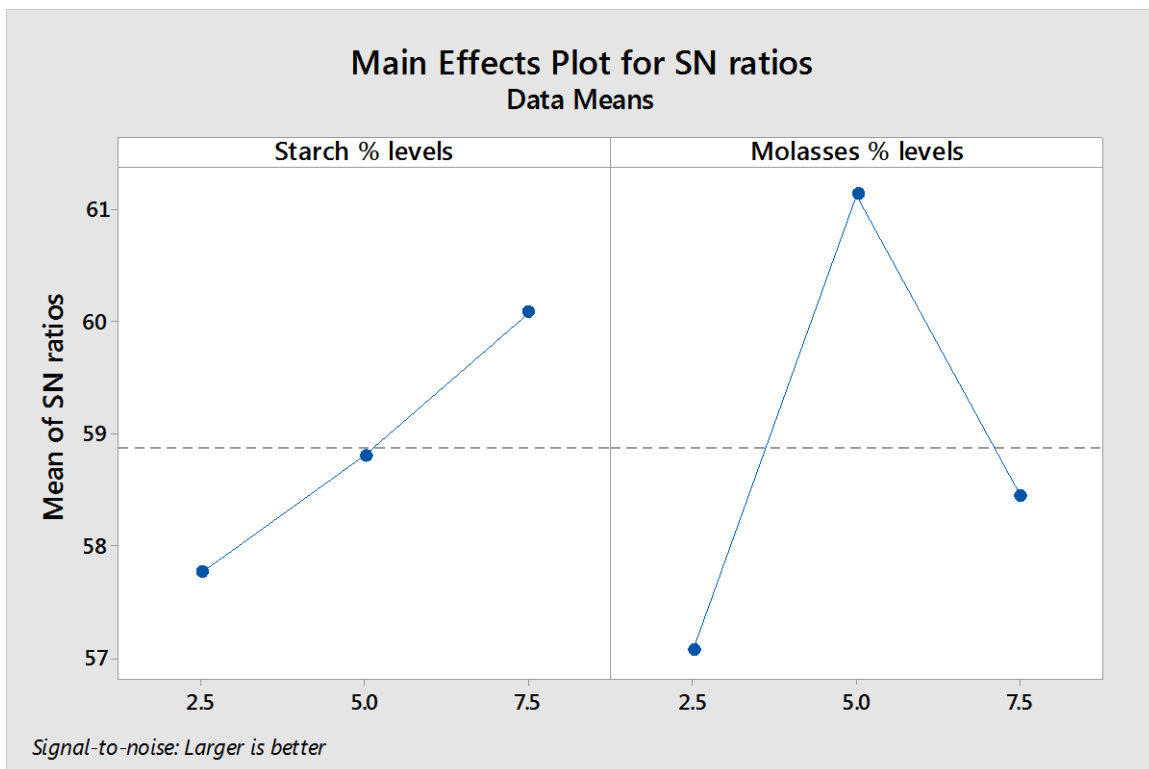


**Fig. 4.6: Individual plot of signal to noise ratio for strength**

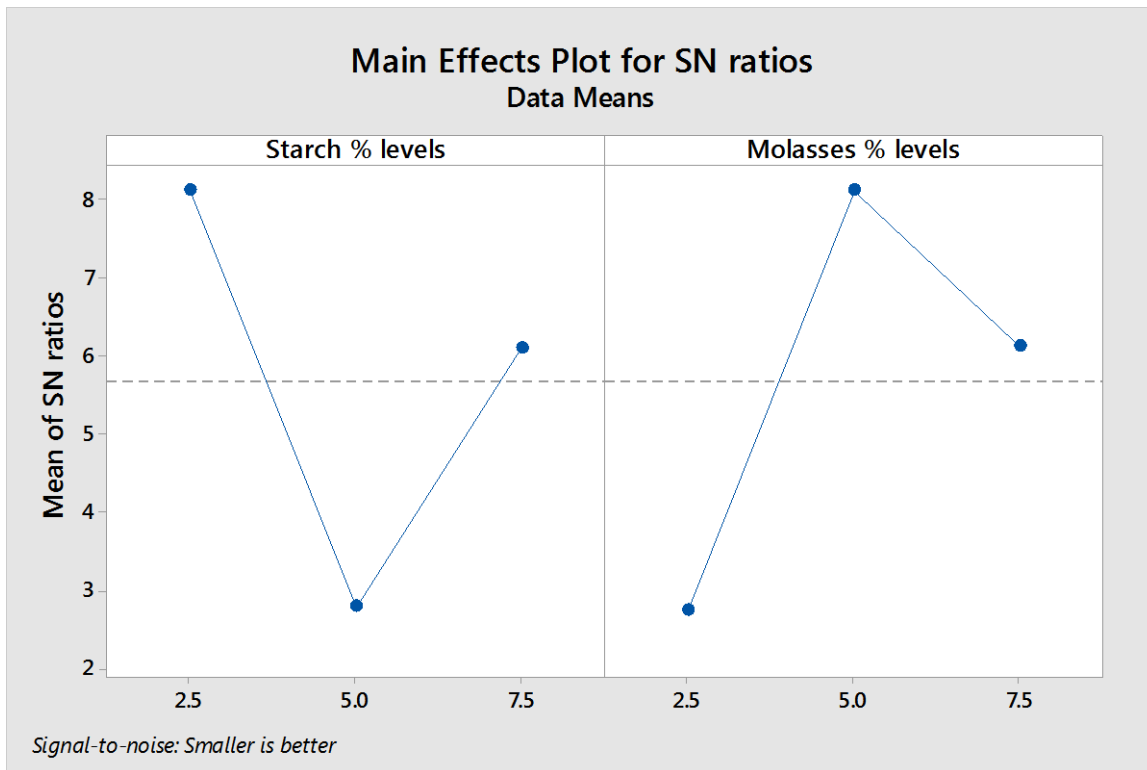


**Fig. 4.7: Individual plot of Signal to Noise for shatter index**

From Figure 4.6 which is for signal to noise ratio of strength, with increase in starch percentage, it shows upward trend. While increase in molasses percentage gives maximum reading at 5pct and reduces there on. Figure 4.7 which is for S/N ratio for shatter index, shows that with increase in starch percentage, it shows downward trend initially and then elevates, while with increase in molasses percentage, graph shows upward trend up to 5pct then declines. This implies that for 5pct starch to have maximum noise and with 5pct molasses to have minimum noise; so starch is better either 2.5pct or 7.5pct and molasses any value beyond 2.5pct.

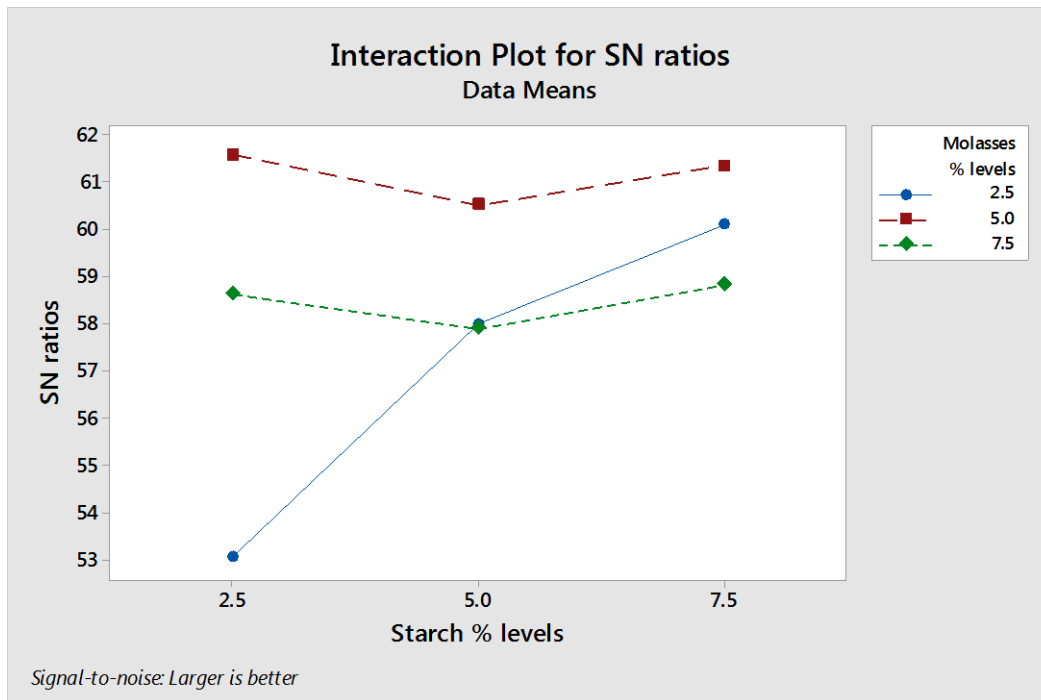


**Fig. 4.8: Interaction plot of Signal to Noise ratio for briquette strength**

Figure 4.8 is the interaction plot of signal to noise ratio for all different combinations of binder percentages for strength. Large S/N ratio shows large signals and low noise which ultimately refers to more reliable combination of the two binders.

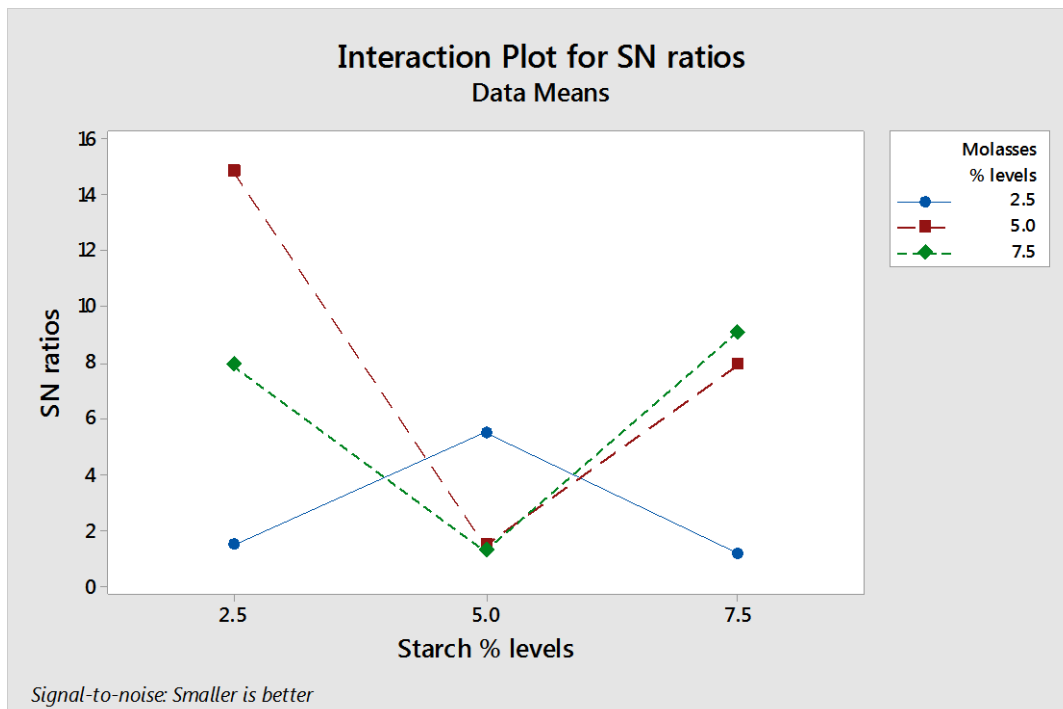


**Fig. 4.9: Interaction plot of Signal to Noise ratio for shatter index**

Figure 4.9 is the interaction plot of signal to noise ratio for all different combinations of binder percentages for shatter index. Here also, same results are obtained as discussed in the

interaction plot of data means for shatter index (Figure 4.5).

S/N ratio graph shows that with 2.5pct starch and 5pct molasses gives the best result. For 5pct starch none of the molasses combination is good as noise is more and hence S/N ratio is small. Further 7.5pct starch gives best result with 7.5pct and 5pct molasses as low noise of system is always better. Large S/N ratio shows large signals and low noise which ultimately refers to more reliable combination.

The aim was to select optimum combination of the binder percentages for the higher strength and low shatter index. Following shows the ranking tables for both desired properties individually as well as considering both simultaneously.

All the waste had different characteristic and hence trial was done using Taguchi technique with three levels and three variables. To do that L9 orthogonal array for 3x3 is designed using MINITAB software. Table 4.13 presents the three variable and their levels. The experiment runs are generated using MINITAB statistical software is presented in Table 4.14.

**Table 4.13: Selected parameters and their levels for 3X3**

<b>Parameters</b>	<b>Level-1</b>	<b>Level-2</b>	<b>Level-3</b>
Binder-S (Starch)	2.5pct	5.0 pct	7.5pct
Binder-M (Molasses)	2.5pct	5.0 pct	7.5pct
Raw Material**	1	2	3

\*\* Raw Material: 1 → JSW Dust, 2 → JSW Sludge, and 3 → VIZAG Sludge

The experiments were conducted as per the Table 4.14 and results for strength and shatter index are shown in Table 4.15. The ranking is done considering both the output parameter and result is presented in Table 4.16.

**Table 4.14: L9 orthogonal array for 3X3**

<b>Batch No.</b>	<b>Raw Material</b>	<b>Starch pct</b>	<b>Molasses pct</b>
EE1	1	2.5	2.5
EE2	2	2.5	5.0
EE3	3	2.5	7.5
EE4	2	5.0	2.5
EE5	3	5.0	5.0
EE6	1	5.0	7.5
EE7	3	7.5	2.5
EE8	1	7.5	5.0
EE9	2	7.5	7.5

**Table 4.15: L9 orthogonal array results for 3x3**

<b>Experiment Run</b>	<b>Starch (pct)</b>	<b>Molasses (pct)</b>	<b>Raw Material</b>	<b>Strength (N/Briquette)</b>	<b>Shatter Index (pct)</b>
EE1	2.5	2.5	1	451.26	0.84
EE2	2.5	5.0	2	539.0	2.096
EE3	2.5	7.5	3	960.4	0.636
EE4	5.0	2.5	2	1435.7	1.488
EE5	5.0	5.0	3	759.5	0.529
EE6	5.0	7.5	1	784.8	0.86
EE7	7.5	2.5	3	1063.3	0.358
EE8	7.5	5.0	1	1167.39	0.4
EE9	7.5	7.5	2	1014.3	0.064

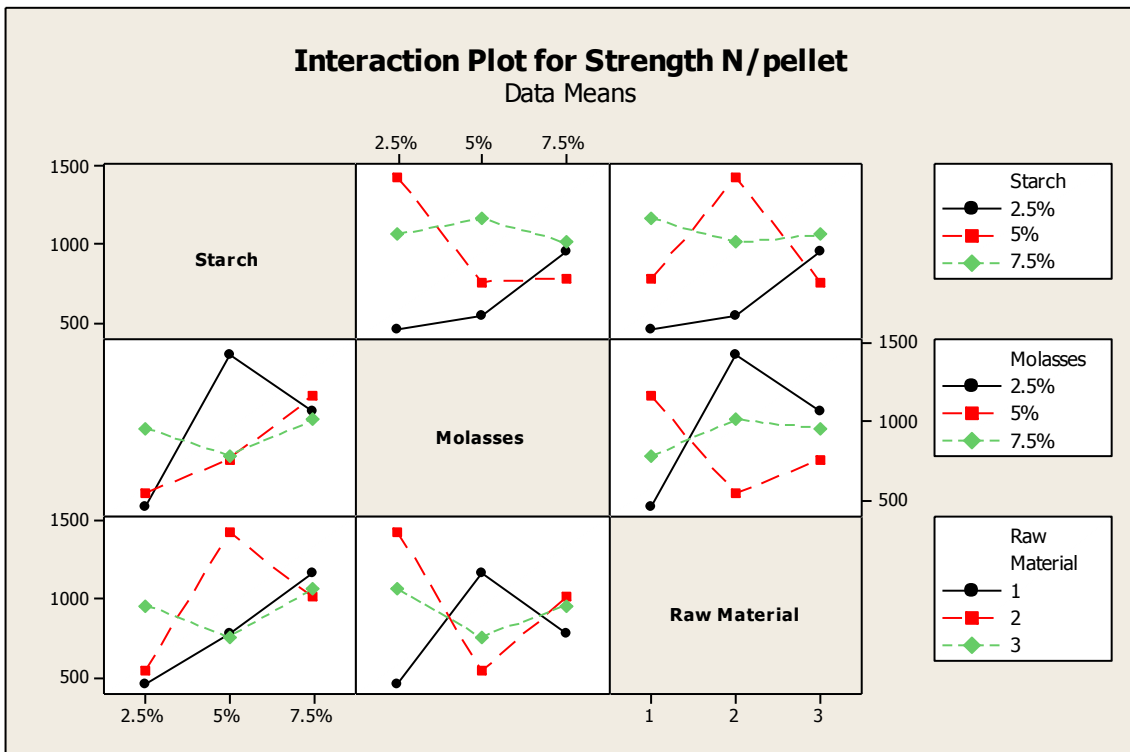


**Fig. 4.10: Interaction plot for strength**

Figure 4.10 shows the interaction plot for strength. 7.5pct starch individually gives higher strength values. 7.5pct molasses shows promising and consistent values of strengths however 2.5pct molasses gives maximum strength value with 5.0 pct starch and raw material-2(i.e. JSW Sludge). Raw material-1 (i.e. JSW Dust) has inconsistent strength values while raw material-3 (i.e. VIZAG Sludge) has consistent values.

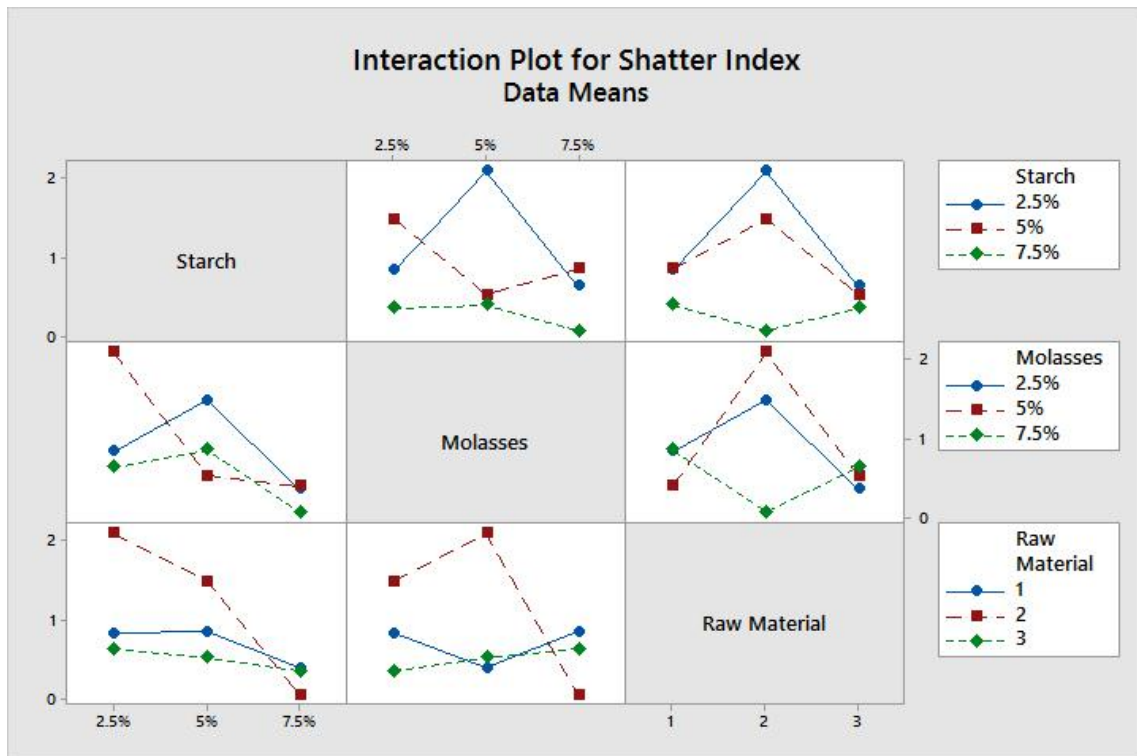


**Fig 4.11: Interaction plot for shatter Index**

Figure 4.11 shows the interaction plot for shatter index. 7.5pct starch as well as 7.5pct molasses individually gives low shatter index readings consistently. Also, raw material-3 (i.e. VIZAG Sludge) shows low shatter index values individually. Raw material-2 (i.e. JSW Sludge) gives higher shatter indexes which is not desirable.

i) Weighted index for strength =  $\frac{\text{Particular strength}}{\text{Max.strength}}$  ... (4.13)

e.g. for EE9: Weighted index for strength =  $[1014.3/1435.7] = 0.7065$

ii) Weighted index for shatter index =  $\frac{\text{Min.shatter index}}{\text{Particular shatter index}}$  ... (4.14)

e.g for EE4 : Weighted index for Shatter index =  $[0.064/1.488] = 0.043$

iii) Total Index=(Weighted index for strength + Weighted index for shatter index) .... (4.15)

**Table 4.16: Ranking order considering effect of both outputs**

Rank	Experiment Run	Starch (pct)	Molasses (pct)	Raw Material	Strength (N/Briquette)	Shatter Index (pct)	Weighted index for strength	Weighted index for Shatter index	Total Index
1	EE9	7.5	7.5	2	1014.3	0.064	0.7065	1	1.7065
2	EE4	5.0	2.5	2	1435.7	1.488	1	0.043	1.043
3	EE8	7.5	5.0	1	1167.39	0.4	0.8131	0.16	0.9731
4	EE7	7.5	2.5	3	1063.3	0.358	0.7406	0.1788	0.9194
5	EE3	2.5	7.5	3	960.4	0.636	0.6689	0.1006	0.7695
6	EE5	5.0	5.0	3	759.5	0.529	0.529	0.121	0.65
7	EE6	5.0	7.5	1	784.8	0.86	0.5466	0.0744	0.621
8	EE2	2.5	5.0	2	539.0	2.096	0.3754	0.0305	0.4059
9	EE1	2.5	2.5	1	451.26	0.84	0.3143	0.0762	0.3905

Weighted index for the individual outcome for strength and shatter index also for combined properties for pellets are calculated and using that information. Proper combination of starch and molasses, as per required strength and/or shatter index, is selected. Strength and shatter index are complementary properties for pellet. Significance of both the properties may be a compromise between the two. With the help of the Table 4.16, the combination of the two properties according to the rank, finally the proportion of the binder can be selected.

### 4.3 Bonding Mechanism

#### 4.3.1 Corn Starch

The general chemical formula of corn starch is  $[(C_6H_{10}O_5)_n]$ . Corn starch has semi-crystalline particle structure, the internal area is non-crystalline, while the outer area is crystallized (as shown in Figure 4.12). At the same time, the high relative molecular mass of corn starch and the close reticular formation generated from hydroxyl synthesis by hydrogen bond result in high viscosity[116]. By adding water to the corn starch, swelling take place and viscosity increases; so, the briquettes get a high strength at room temperature. With the temperature rising, the water molecules enter the corn starch, combine with starch molecular and start irreversible swell. When the temperature reaches 110°C, the gelatinization (i.e. it is a process of breaking down the intermolecular bonds of starch molecules in the presence of water and heat) is completed. The original morphological structure of corn starch granules is broken, and the intermolecular interaction is weakened, due to that thoroughly starch spread on the waste

concentrate and coal particles. At 200°C corn starch gradually transforms into a continuous solid bridge formation (Figure 4.13), which connected the concentrate and coal particles closely and strength of the composite briquettes increases. Because of mechanical force, the crystal structure of corn starch has been destroyed. The degree of lattice ordering of crystal in crystalline area reduces gradually, which creates a good fluidity of corn starch.

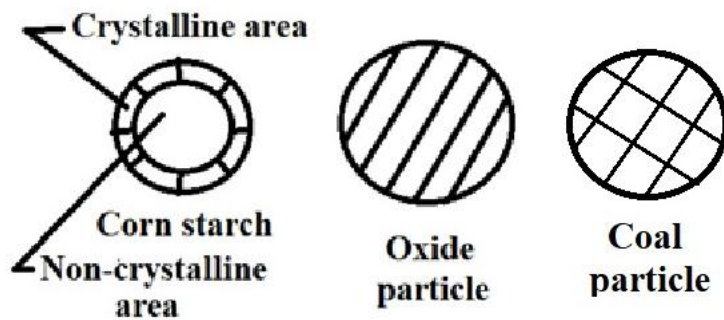


**Fig. 4.12: Corn starch, waste concentrate and coal particles**

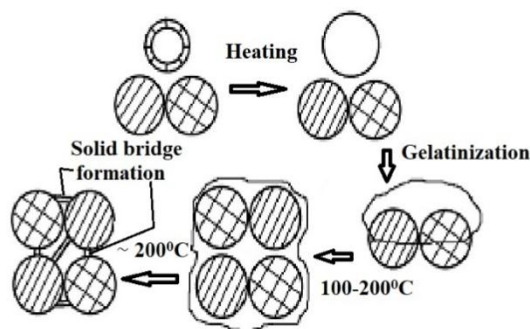


**Fig. 4.13: Bonding mechanism of corn starch**

Corn starch can improve the composite briquettes strength at room temperature and the strength after drying because of the expansibility after absorbing water and compatibility after gelatinization of corn starch. At 100-200°C corn starch thoroughly spreads on the waste concentrate and coal particles and after 200°C corn starch gradually transforms into a continuous solid bridge formation, which connected the concentrate particles and coal particles closely. The strength of composite briquettes/pellets are improved.

### 4.3.2 Corn starch and Molasses

Molasses is a viscous product resulting from refining sugarcane or sugar beets into sugar. Molasses (containing around 50 pct fermentable sugars and 80 pct soluble



#### 4.4 Pellets Preparation

Figure 4.15 shows the flow diagram for composite pellet making. Binders were selected based on briquettes formation and proper strength of briquettes. Waste-coal composite pellets were prepared using as binder based on Table 4.16, binder proportions (i.e. starch and molasses) were selected for all the three raw materials (Table 4.17) and bulk pellets were prepared according to their compositions (Table 4.18).

**Table 4.17: Selection of binder for pellets**

<b>Raw Material</b>	<b>Starch, pct</b>	<b>Molasses, Pct</b>
JSW Dust (1)	7.5	5.0
JSW Sludge(2)	5.0	2.5
VIZAG Sludge (3)	7.5	2.5

**Table 4.18: Composition of composite pellets**

S.No.	Composition	Weight, g	Pct
1a.	JSW Dust	1000	69.35
1b.	Coal (stoichiometric)	317	21.98
1c.	Binder (7.5 pct starch + 5 pct molasses)	125	8.67
2a.	JSW Sludge	1000	71.22
2b.	Coal	329.1	23.44
2c.	Binder (5 pct starch + 2.5 pct molasses)	75	5.34
3a.	VIZAG Sludge	1000	70.86
3b.	Coal	311.3	22.06
3c.	Binder (7.5 pct starch + 2.5 pct molasses)	100	7.08

First mixing of raw materials(waste fines, coal fines, and binders) were done in a porcelain jar rotated at 50 rpm for one hour in a pebble mill. Pellets were prepared in batches using a disc pelletizer (400 mm diameter and 40° angle of pelletizer ) which rotated at 17 rpm . The mixture was fed into the disc manually and water was added by spraying time to time. Total moisture was in the range of 8 to 10 pct by weight of the mixture. The green pellets of nearly 12 to 22 mm sizes were formed. CO<sub>2</sub> gas were not passed to the pellets for hardening. The pellets were dried in open atmosphere for 24 hours. These pellets got hardened in cold bonding process due to physico-chemical changes of the binder in ambient condition. For experimental work, composite pellets were prepared using coals from local sources having Fe<sub>tot</sub>/C ratio as per stoichiometric.

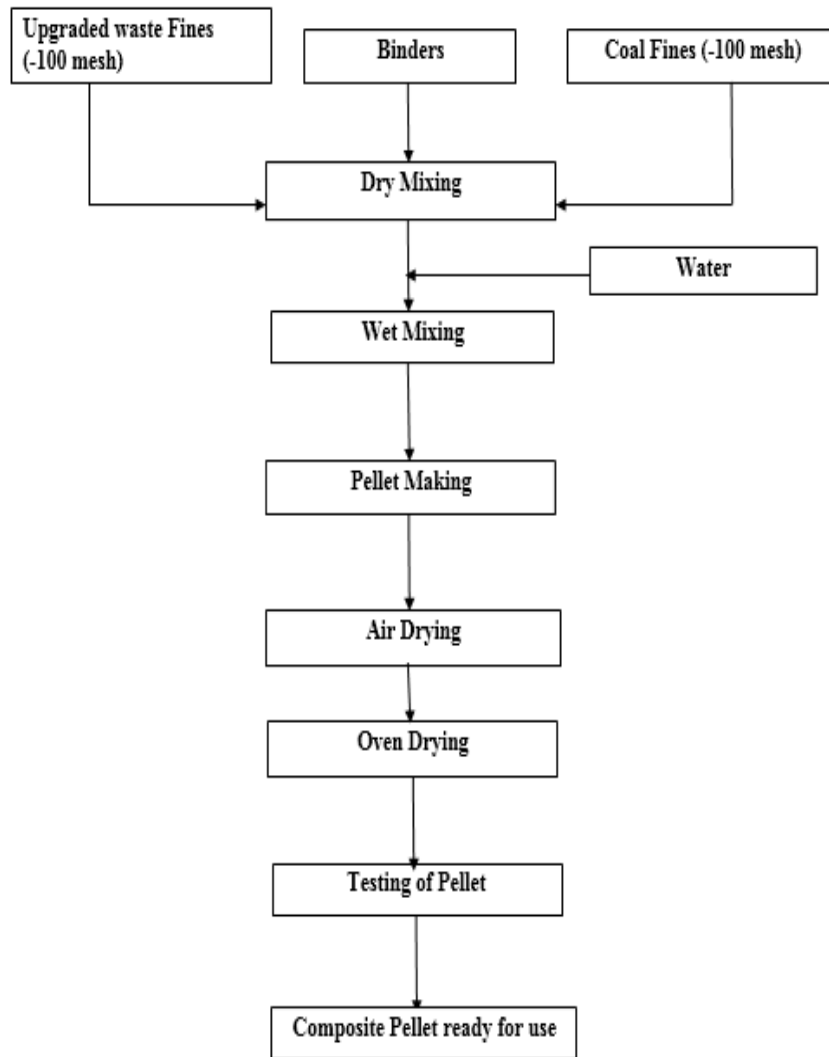


**Fig.4.15:Flow diagram of composite pellet making**

## 4.5 Study of Reducibility

The degree of reduction of iron oxide can be obtained by reducibility studies through weight loss method, when a gaseous reductant is used. For reduction of iron oxides by carbon, the degree of reduction cannot be found out directly from the weight loss of the sample, since both oxygen and carbon are loosed during reduction. It is not possible to delineate the two unless the released gases are analyzed and their volumes are measured. Accordingly, such reactions have been studied with the help of gas chromatograph attached with the reduction chamber. Even this method runs into trouble when coal is used in place of pure carbon or graphite. Alternatively, the reaction product can be chemically analyzed after each test run, but this procedure is time consuming, more expensive and gives only intermittent information. For ore-coal composite pellets, the weight loss of the sample arises not only from oxygen and carbon loss, but also the loss of volatile matters and residual moisture present in pellets[13]. Since only weight loss of the sample is not sufficient, some additional measurements are required for estimating the degree of reduction ( $\alpha$ ), which is defined as follows:

$$\alpha = \frac{\text{Weight of oxygen removed from iron oxide}}{\text{Total weight of removable oxygen present in iron oxide}} \times 100 \quad \dots(4.21)$$

Sah and Dutta[96] used the following equation for calculation of fraction of reduction to take care of the loss of volatile matters:

$$f = \left[ \frac{4 \times \{f_{wl} - (f_{coal} \times f_{vm})\}}{7 \times (f_{ore} \times \rho_{ore} \times f_o)} \right] \quad \dots(4.22)$$

where,  $f_{wl}$  is fractional weight loss, =  $[(W_i - W_f) / W_i]$ ,

$W_i$  is the initial weight of the composite pellet,

$W_f$  is the final weight of the composite pellet after reduction,

$f_{coal}$  is fraction of coal present in composite pellet,

$f_{vm}$  is fraction of volatile matters present in coal,

$f_{ore}$  is fraction of waste present in composite pellet,

$\rho_{ore}$  is purity of iron oxide ( $Fe_2O_3$ ) in waste,

$f_o$  is fraction of oxygen present in pure  $Fe_2O_3$ .

### 4.5.1 Horizontal Tube Furnace

Electrically heated tube furnace was used for reducibility studies. Temperature was controlled by a Pt-Rh thermocouple. Figure 4.16 shows the set-up for reducibility studies of composite pellets. Fused quartz tube of diameter 20 mm and length 600 mm was used for the reduction. One end of the tube was connected to the nitrogen gas cylinder for creating inert atmosphere

during reduction while the other end of the tube was connected to the water beaker to check the flow of gas. The quartz heating tube was calibrated along the length using Pt-Rh thermocouple to assess the perfect reaction zone within the tube.



**Fig. 4.16: Experimental set-up for isothermal reduction of composite pellets**



**Fig.4.17: Ceramic boat for samples of reducibility studies**

The experiments were designed to investigate the reduction kinetics of the composite pellets in isothermal condition at various temperature. Special alumina boat (18 x 18 x70 mm) was prepared for the pellets to be placed into the tube furnace. Pellets were dried at 150<sup>0</sup>C for 30 minutes before placing it into the furnace. Two pellets of 12-15 mm diameter were taken simultaneously. Pellets were weighed using electronic balance of 0.001g accuracy. The weights of pellets were in the range of 3 to 7 g. The pellets were placed in high alumina boat (Figure4.17), which was put into the preheated tube furnace in nitrogen(99.5% pure) atmosphere. The reaction time was noted and after reduction the boat was shifted to the cooling zone of the tube and allowed to cool the pellets in the nitrogen atmosphere for 5 minutes. Then the reduced pellets were transferred to the desiccators for further cooling. The cooled pellets were weighted to calculate the fraction of reduction. The variables for Isothermal reduction of composite pellets are shown in Table 4.19.

**Table 4.19: Variables for isothermal reduction of composite pellets**

Sr.No.	Variable	Number	Remarks
1	Steel plant Waste	3	JSW Dust, JSW Sludge, VIZAG Sludge
2	Coal	1	From local market
3	Temperature (°C)	3	950, 1000 and 1050
4	Time (s)	5	150, 300, 450, 600 and 1200

#### 4.5.2 Measurement of Rate of Reduction (k) and Activation Energy (E)

The fraction of reduction (f) of composite pellets are calculated as per eq. (4.22). Then, f vs t plots are drawn. From the initial straight line of the plot, the slope of the line is found out to know the rate of reduction (k).

Therefore, 
$$k = \frac{df}{dt} \quad \dots(4.23)$$

From the rate of reduction (k), the activation energy (E) can be calculated from Arrhenius equation:

$$\text{Rate, } k = A \cdot e^{-(E/RT)} \quad \dots (4.24)$$

where A is constant, E is activation energy, R is gas constant, and T is absolute temperature.

Therefore, 
$$\ln k = \ln A - (E/RT) \quad \dots (4.25)$$

Equation (4.25) is used in analyzing the reduction kinetic data. A plot of ln k vs 1/T gives slope (E/R) and from the slope of the line, the activation energy (E) can be estimated.

Therefore, the activation energy (E) = [slope x R] 
$$\dots (4.26)$$

## 4.6 Results for Reduction of Composite

### 4.6.1 Results for JSW Dust

The composition for JSW dust composite pellet is shown in Table 4.18. JSW Dust contains 87.33 pct  $\text{Fe}_2\text{O}_3$  after beneficiation. Tables 4.20 to 4.22 show the reduction data for JSW Dust composites. Figures 4.18 to 4.20 show the reduction curves for JSW Dust composites. Detail calculations of fraction of reduction (f) are shown in Appendix 1.

**Table 4.20: Reduction data for JSW Dust composite at 950°C**

Time, s	Initial weight, g ( $W_1$ )	Final weight, g ( $W_2$ )	Diff. in weight, g ( $W_1 - W_2$ )	Fractional weight loss, ( $f_{wl}$ ) [( $W_1 - W_2$ ) / $W_1$ ]	Fraction of reduction, f [as per Eq. (4.14)]	Avg. f
300	4.369	4.149	0.2200	0.0504	0.0410	0.0387
300	4.112	3.911	0.2010	0.0489	0.0363	
450	4.838	4.528	0.3100	0.0641	0.0841	0.0808
450	3.548	3.328	0.2200	0.0620	0.0775	
600	3.359	3.136	0.2230	0.0664	0.0913	0.0895
600	2.947	2.755	0.1920	0.0652	0.0876	
1200	3.384	3.128	0.2560	0.0757	0.1206	0.1106
1200	3.433	3.195	0.2380	0.0693	0.1005	

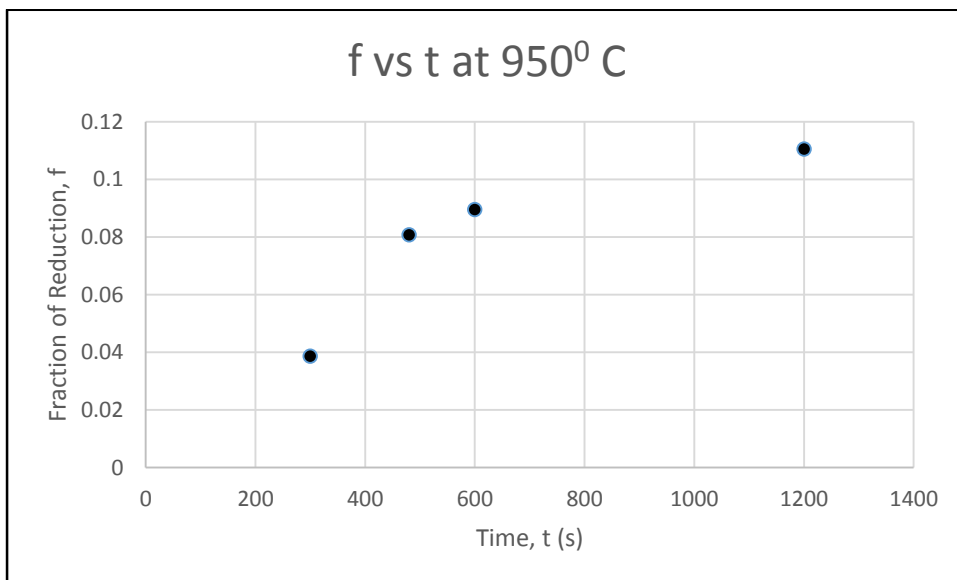


**Fig.4.18: Reduction curve for JSW Dust composite at 950°C**

**Table 4.21: Reduction data for JSW Dust composite at 1000°C**

Time,s	Intial weight, g( $W_1$ )	Final weight, g ( $W_2$ )	Diff. in weight, g ( $W_1 - W_2$ )	$f_{wl}$ fractional weight loss, $[(W_1 - W_2) / W_1]$	Fraction of reduction, $f$ [as per Eq.(4.14)]	Avg. $f$
180	3.507	3.302	0.2050	0.0585	0.0665	0.0690
180	3.978	3.739	0.2390	0.0601	0.0715	
300	3.945	3.656	0.2890	0.0733	0.1130	0.1058
300	3.462	3.224	0.2380	0.0687	0.0986	
450	4.128	3.784	0.3440	0.0833	0.1445	0.1333
450	3.845	3.552	0.2930	0.0762	0.1222	
600	4.761	4.269	0.4920	0.1033	0.2074	0.1807
600	5.108	4.667	0.4410	0.0863	0.1539	
1200	4.423	3.928	0.4950	0.1119	0.2344	0.2377
1200	4.921	4.360	0.5610	0.1140	0.2410	

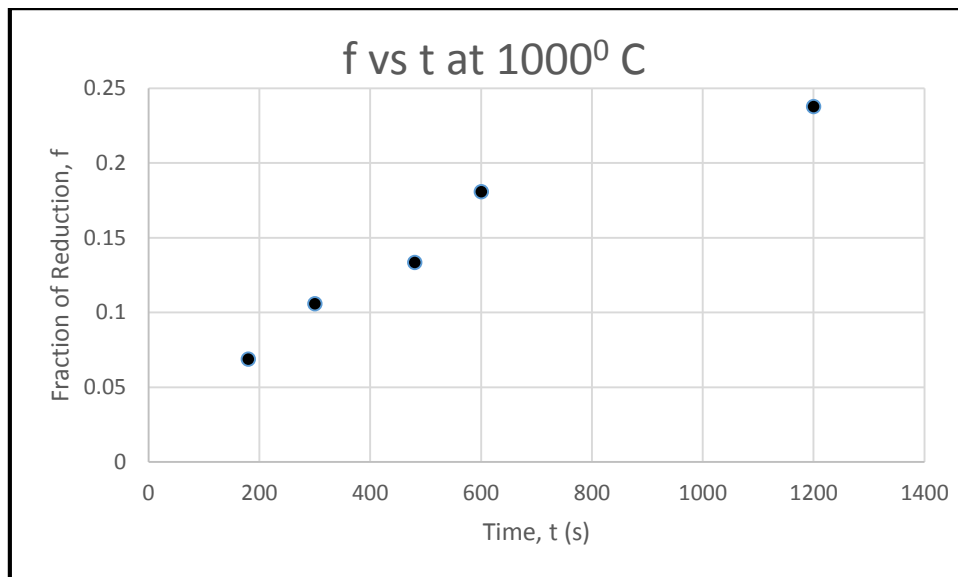


**Fig. 4.19: Reduction curve for JSW Dust composite at 1000°C**

**Table 4.22: Reduction data for JSW Dust composite at 1050°C**

Time, s	Initial weight, g( $W_1$ )	Final weight, g( $W_2$ )	Diff. in weight, g ( $W_1 - W_2$ )	$f_{wl}$ fractional weight loss, $[(W_1 - W_2) / W_1]$	Fraction of reduction, f [as per Eq. (4.14)]	Avg.f
150	3.898	3.660	0.2380	0.0611	0.0747	0.05
150	3.990	3.809	0.1810	0.0454	0.0253	
300	3.357	3.171	0.1860	0.0554	0.0567	0.0592
300	3.248	3.063	0.1850	0.0570	0.0618	
450	4.183	3.797	0.3860	0.0923	0.1728	0.1786
450	3.926	3.549	0.3770	0.0960	0.1844	
600	4.412	3.966	0.4460	0.1011	0.2005	0.2016
600	3.831	3.441	0.3900	0.1018	0.2027	
1200	3.244	2.747	0.4970	0.1532	0.3643	0.3415
1200	2.928	2.522	0.4060	0.1387	0.3187	

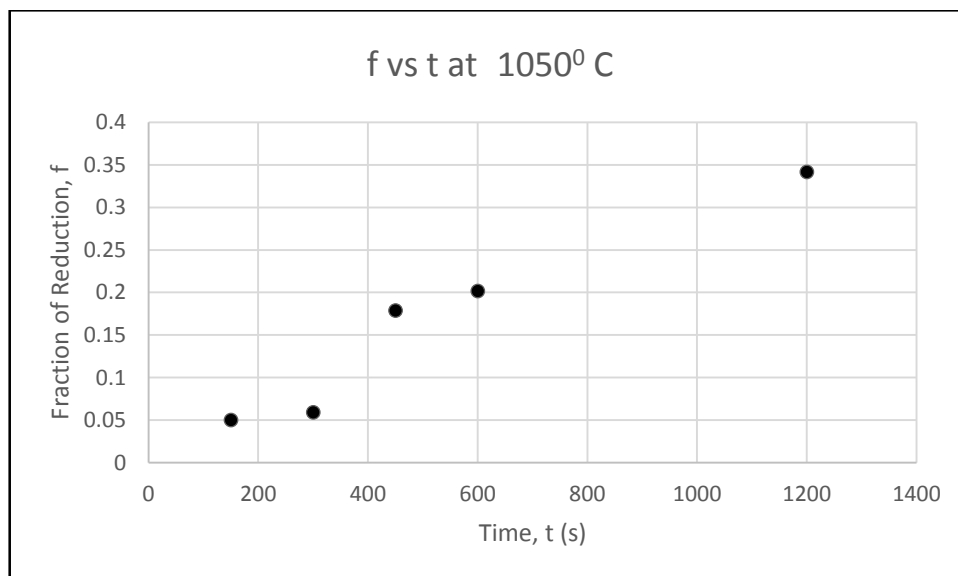


**Fig. 4.20: Reduction curve for JSW Dust composite at 1050°C**

**Table 4.23: Rate of reduction for JSW Dust composite at various temperatures**

Sr.no.	Temp (°C)	Temp (K)	$(1/T) \times 10^4$	Rate, k $\times 10^4$	$\ln k$
1	950	1223	8.18	2.27	-8.39
2	1000	1273	7.86	3.08	-8.09

3	1050	1323	7.56	3.37	-8.00
---	------	------	------	------	-------

Figure 4.21 shows the reduction curves at various temperatures for JSW Dust composite. From the Figure 4.21, the fraction of reduction increases with increasing in temperature and time. The rate of reduction for JSW Dust at various temperatures are shown in Table 4.23.  $\ln k$  vs  $1/T$  is plotted for JSW Dust composite (Figure 4.22) and the slope of the line is found out to calculate activation energy. The activation energy for JSW Dust composite is found to be 52.59 KJ/mol.

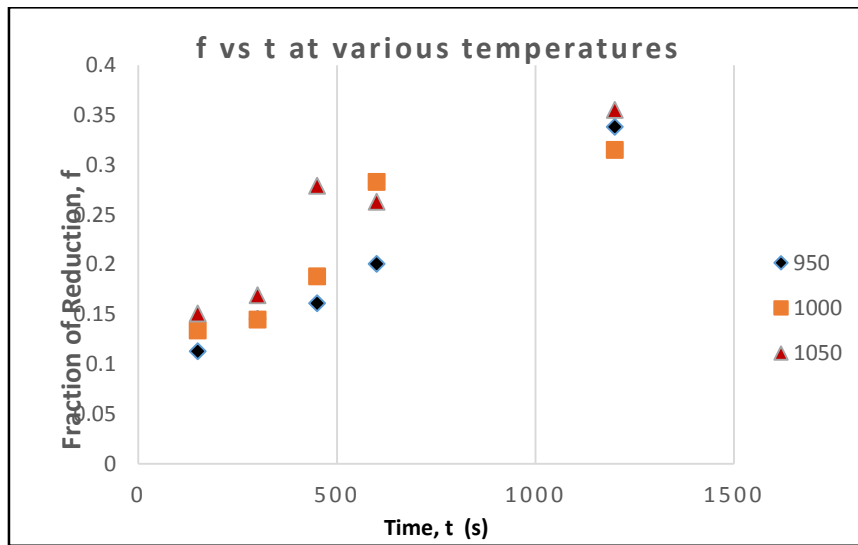


**Fig. 4.21: Reduction curves at various temperatures for JSW Dust composite**

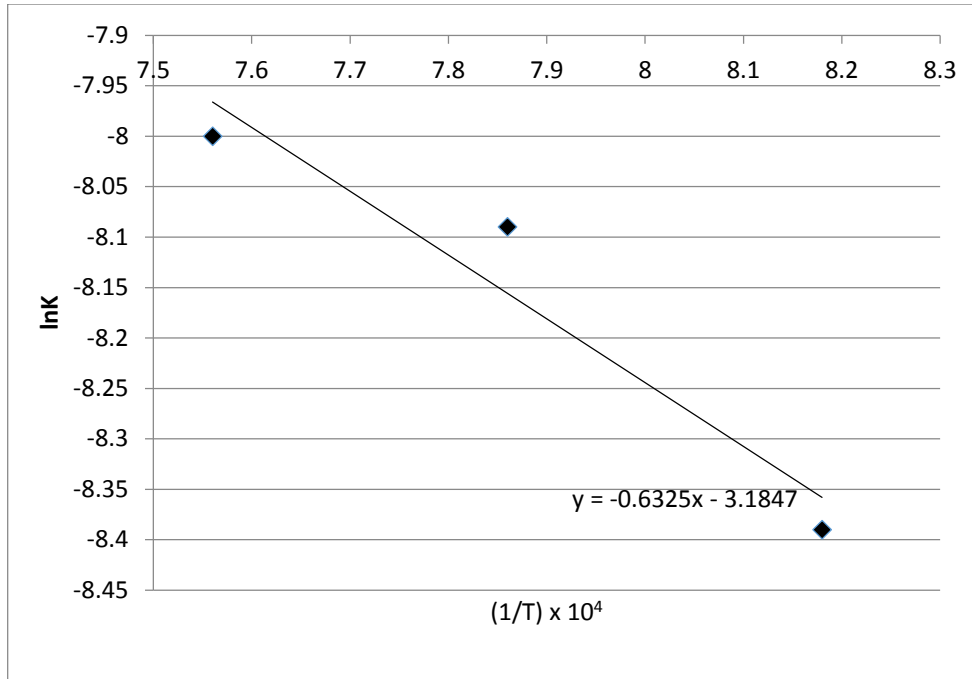


**Figure 4.22 : Arrhenius plot for JSW Dust composite**

#### 4.6.2 Results for JSW Sludge

The composition for JSW Sludge composite pellet is shown in Table 4.18. JSW Sludge contains 90.69 pct Fe<sub>2</sub>O<sub>3</sub> after beneficiation. Tables 4.24 to 4.26 show the reduction data for JSW Sludge composites. Figures 4.23 to 4.25 show the reduction curves for JSW Sludge composites. Detail calculations of fraction of reduction (f) are shown in Appendix 1.

**Table 4.24: Reduction data for JSW Sludge composite pellet at 950°C**

Time, s	Initial weight, g(W <sub>1</sub> )	Final weight, g(W <sub>2</sub> )	Diff. in weight, g (W <sub>1</sub> -W <sub>2</sub> )	f <sub>wl</sub> fractional weight loss, [(W <sub>1</sub> - W <sub>2</sub> ) / W <sub>1</sub> ]	F	Avg. f
150	7.245	6.648	0.5970	0.0824	0.1256	0.1131
150	6.900	6.390	0.5100	0.0739	0.1005	
300	6.876	6.257	0.6190	0.0900	0.1480	0.1455
300	6.956	6.342	0.6140	0.0883	0.1430	
450	6.433	5.825	0.6080	0.0945	0.1613	0.1613
600	5.988	5.373	0.6150	0.1027	0.1855	0.2008
600	6.836	6.063	0.7730	0.1131	0.2161	
1200	6.469	5.526	0.9430	0.1458	0.3126	0.3384

1200	6.700	5.606	1.0940	0.1633	0.3642	
------	-------	-------	--------	--------	--------	--

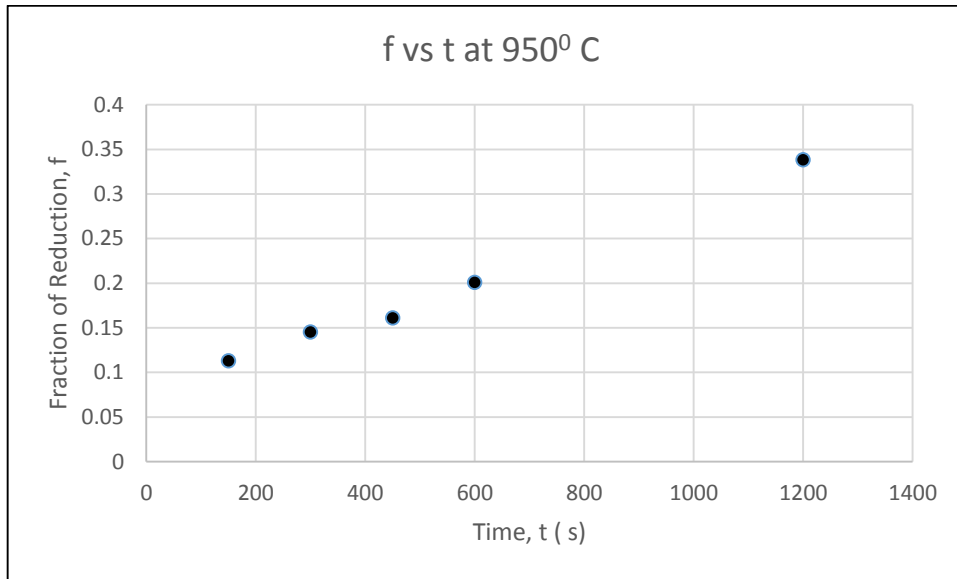


**Fig. 4.23:Reduction curve for JSW Sludge composite at 950° C**

**Table 4.25: Reduction data for JSW Sludge composite pellet at 1000°C**

Time, s	Initial weight, g( $W_1$ )	Final weight, g( $W_2$ )	Diff. in weight, g ( $W_1 - W_2$ )	$f_w$ fractional weight loss, $[(W_1 - W_2) / W_1]$	F	Avg. f
150	5.164	4.724	0.4400	0.0852	0.1339	0.1680
150	5.622	5.013	0.6090	0.1083	0.2020	
300	5.893	5.346	0.5470	0.0928	0.1563	0.1450
300	5.760	5.270	0.4900	0.0851	0.1336	
450	5.922	5.298	0.6240	0.1054	0.1934	0.1883
450	4.964	4.458	0.5060	0.1019	0.1831	
600	5.803	4.973	0.8300	0.1430	0.3043	0.2831
600	5.134	4.474	0.6600	0.1286	0.2618	
1200	6.643	5.580	1.0630	0.1600	0.3544	0.3152
1200	5.654	4.900	0.7540	0.1334	0.2760	

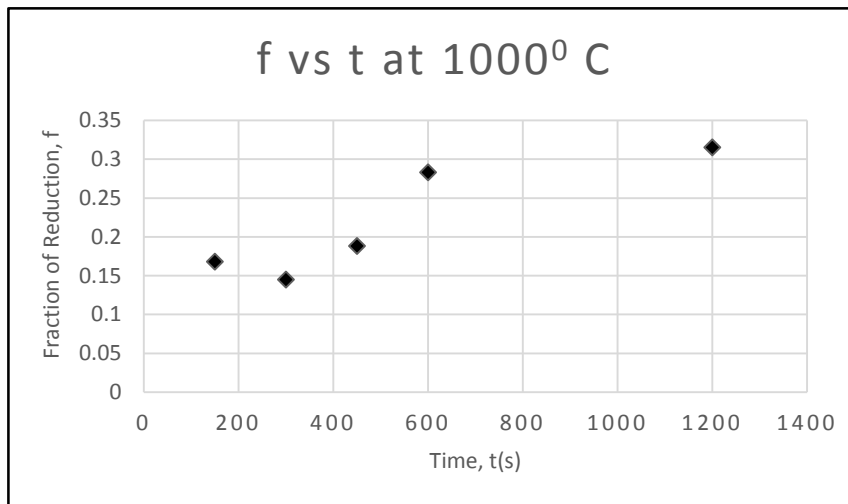


**Fig. 4.24: Reduction curve for JSW Sludge composite at 1000°C**

**Table 4.26: Reduction Data for JSW Sludge Composite Pellet at 1050°C**

Time, s	Initial weight, g( $W_1$ )	Final weight, g( $W_2$ )	Diff. in weight, g ( $W_1 - W_2$ )	$f_{wl}$ fractional weight loss, $[(W_1 - W_2) / W_1]$	F	Avg. f
150	4.664	4.244	0.4200	0.0901	0.1483	0.1511
150	5.400	4.903	0.4970	0.0920	0.1539	
300	4.776	4.260	0.5160	0.1080	0.2011	0.1694
300	5.540	5.061	0.4790	0.0865	0.1377	
450	5.325	4.705	0.6200	0.1164	0.2259	0.2793
450	4.435	3.758	0.6770	0.1526	0.3326	
600	4.312	3.716	0.5960	0.1382	0.2902	0.2713
600	4.641	4.059	0.5820	0.1254	0.2524	
1200	4.035	3.352	0.6830	0.1693	0.3819	0.3554
1200	2.994	2.541	0.4530	0.1513	0.3288	

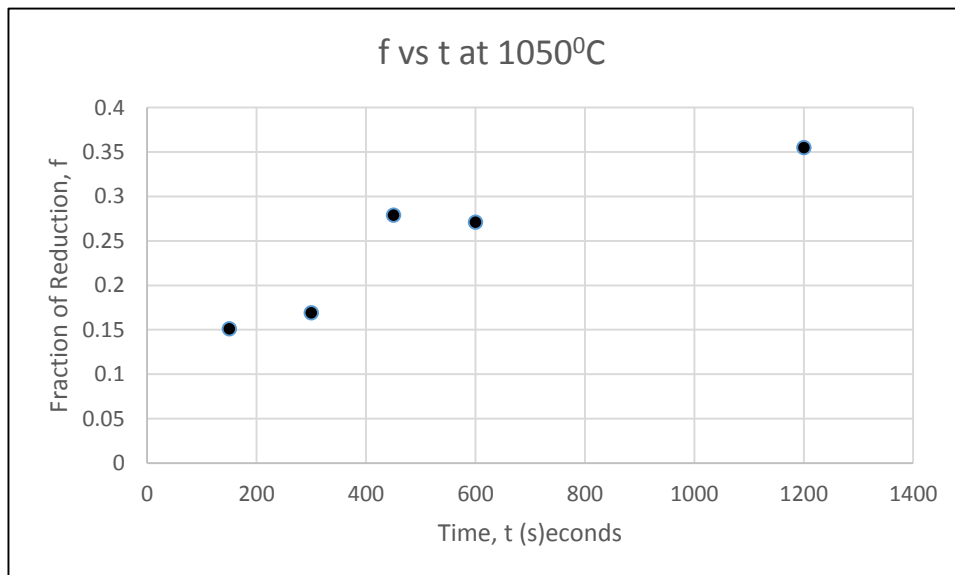


**Fig. 4.25: Reduction curve for JSW Sludge composite at 1050° C**

Figure 4.26 shows the reduction curves at various temperatures for JSW Sludge composite. From the Figure 4.26, the fraction of reduction increases with increasing in temperature and time. The rate of reduction for JSW Sludge at various temperatures are shown in Table 4.27.

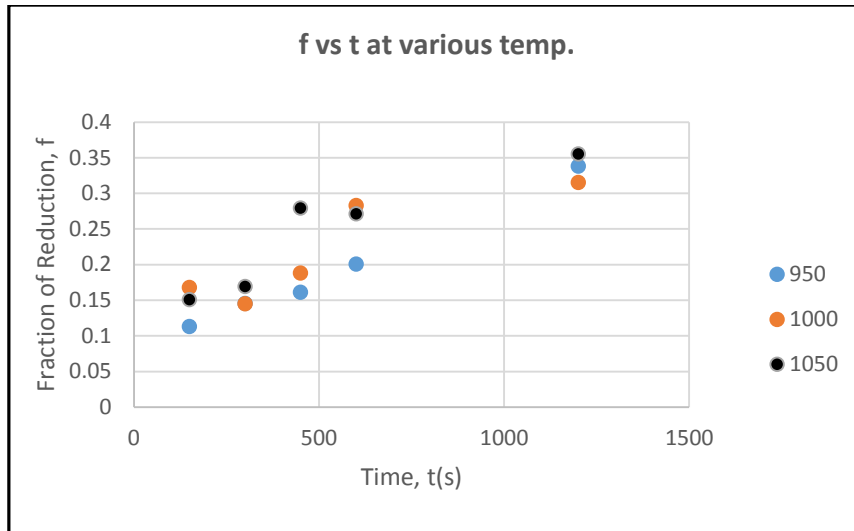


**Fig. 4.26: Reduction curves at various temperatures for JSW Sludge composite**

lnk vs 1/T is plotted (Figure 4.27) for JSW Sludge and the slope of the line is found out to calculate activation energy. The activation energy for JSW Sludge is found to be 49.8 KJ/mol.

**Table 4.27: Rate of reduction for JSW Sludge composite pellet at various temperature**

Sr.no.	Temp	Temp (K)	(1/T) x 10 <sup>4</sup>	Rate, k	Ln k
	(°C)			X 10 <sup>4</sup>	
1	950	1223	8.18	7.08	-7.25
2	1000	1273	7.86	9.33	-6.98
3	1050	1323	7.56	10.26	-6.88

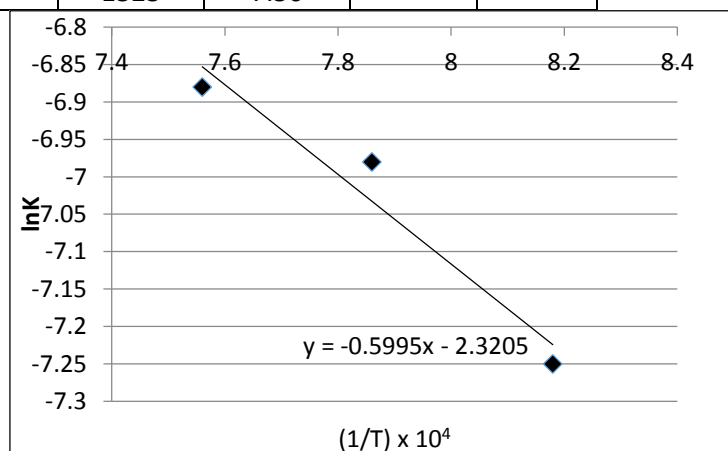


**Fig. 4.27: Arrhenius plot for JSW Sludge**

#### 4.6.3 Results for VIZAG Sludge

The composition for VIZAG Sludge composite pellet is shown in Table 4.18. VIZAG Sludge contains 85.77 pct  $\text{Fe}_2\text{O}_3$  after beneficiation. Tables 4.28 to 4.30 show the reduction data for VIZAG Sludge composites. Figures 4.28 to 4.30 show the reduction curves for VIZAG Sludge composites. Detail calculations of fraction of reduction (f) are shown in Appendix 1.

**Table 4.28: Reduction data for VIZAG Sludge composite pellet at 950°C**

Time, s	Initial weight, g ( $W_1$ )	Final weight, g ( $W_2$ )	Diff. in weight, g ( $W_1 - W_2$ )	$f_{wl}$ fractional weight loss, $[(W_1 - W_2) / W_1]$	F	Avg. f
150	4.840	4.528	0.3120	0.0645	0.0521	0.047
150	4.737	4.448	0.2890	0.0610	0.0412	
300	4.163	3.821	0.3420	0.0822	0.1076	0.1344
300	5.154	4.642	0.5120	0.0993	0.1612	
450	4.606	4.102	0.5040	0.1094	0.1929	0.1987
450	3.519	3.121	0.3980	0.1131	0.2045	
600	3.867	3.277	0.5900	0.1526	0.3282	0.2994
600	3.949	3.419	0.5300	0.1342	0.2706	
1200	3.024	2.560	0.4640	0.1534	0.3308	0.3416
1200	2.807	2.357	0.4500	0.1603	0.3524	

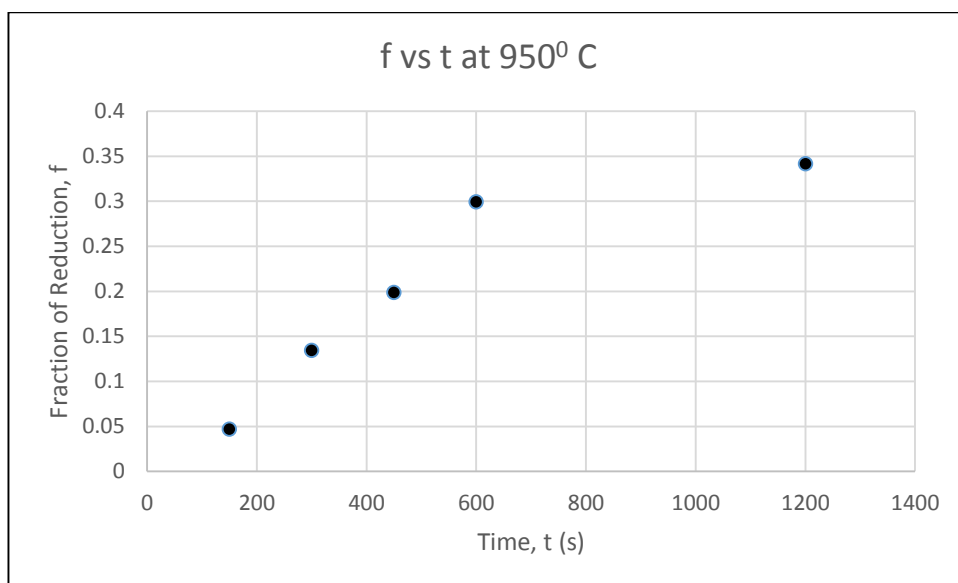


**Fig. 4.28: Reduction curve for VIZAG Sludge composite at 950°C**

**Table 4.29: Reduction data for VIZAG Sludge composite pellet at 1000°C**

Time, s	Intial weight,g( $W_1$ )	Final weight, g( $W_2$ )	Diff. in weight,g ( $W_1 - W_2$ )	$f_{wl}$ fractional weight loss, $[(W_1 - W_2) / W_1]$	f	Avg. f
150	5.174	4.725	0.4490	0.0868	0.1220	0.1286
150	5.046	4.587	0.4590	0.0910	0.1352	
300	4.255	3.859	0.3960	0.0931	0.1418	0.1410
300	3.400	3.085	0.3150	0.0926	0.1402	
450	4.943	4.446	0.4970	0.1005	0.165	0.1661
450	3.953	3.553	0.4000	0.1012	0.1672	
600	5.013	4.309	0.7040	0.1404	0.290	0.2543
600	4.132	3.646	0.4860	0.1176	0.2186	
1200	4.170	3.492	0.6780	0.1626	0.3596	0.3389
1200	4.144	3.525	0.6190	0.1494	0.3182	

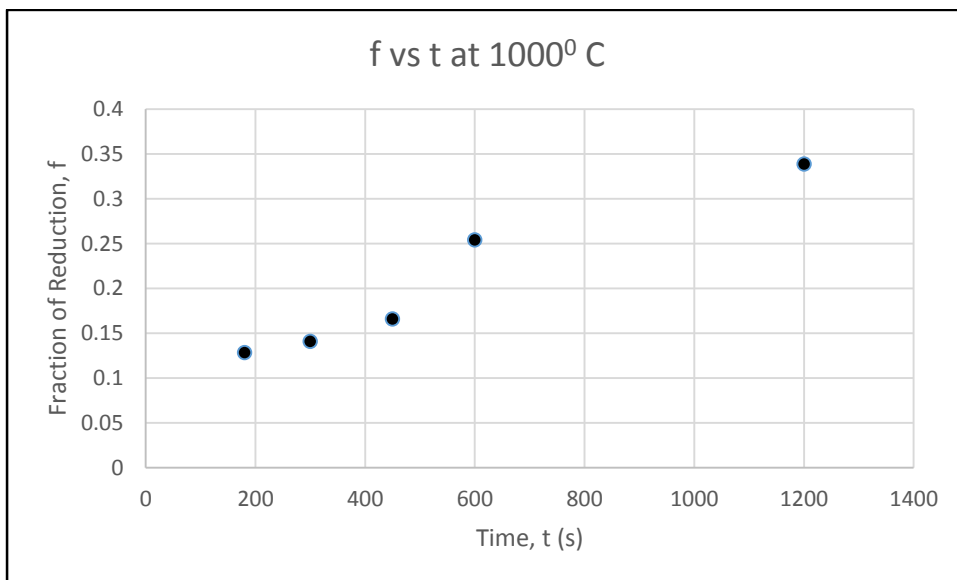


**Fig. 4.29: Reduction curve for VIZAG Sludge composite at 1000°C**

**Table 4.30: Reduction Data for VIZAG Sludge Composite Pellet at 1050°C**

Time, s	Initial weight, g ( $W_1$ )	Final weight, g ( $W_2$ )	Diff. in weight, g ( $W_1 - W_2$ )	$f_{wl}$ fractional weight loss, $[(W_1 - W_2) / W_1]$	f	Avg. f
180	4.867	4.408	0.4590	0.0943	0.1455	0.1592
180	4.417	3.962	0.4550	0.1030	0.1728	
300	4.011	3.432	0.5790	0.1444	0.3025	0.2863
300	4.120	3.568	0.5520	0.1340	0.270	
480	3.535	3.022	0.5130	0.1451	0.3047	0.3055
480	3.715	3.174	0.5410	0.1456	0.3063	
600	4.734	4.019	0.7150	0.1510	0.3232	0.3297
600	4.230	3.574	0.6560	0.1551	0.3361	
1200	3.919	3.194	0.7250	0.1850	0.430	0.3975
1200	3.117	2.605	0.5120	0.1643	0.3649	

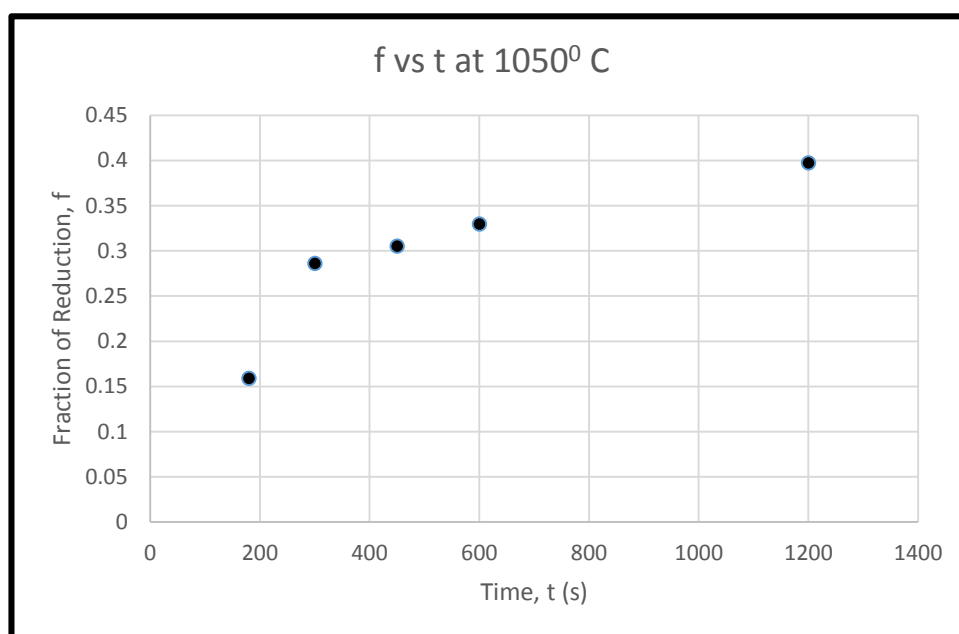


**Fig. 4.30: Reduction curve for VIZAG Sludge composite at 1050° C**

Figure 4.31 shows the reduction curves at various temperatures for VIZAG Sludge composite. From the Figure 4.31, the fraction of reduction increases with increasing in

temperature and time. The rate of reduction for VIZAG Sludge at various temperatures are shown in Table 4.31.

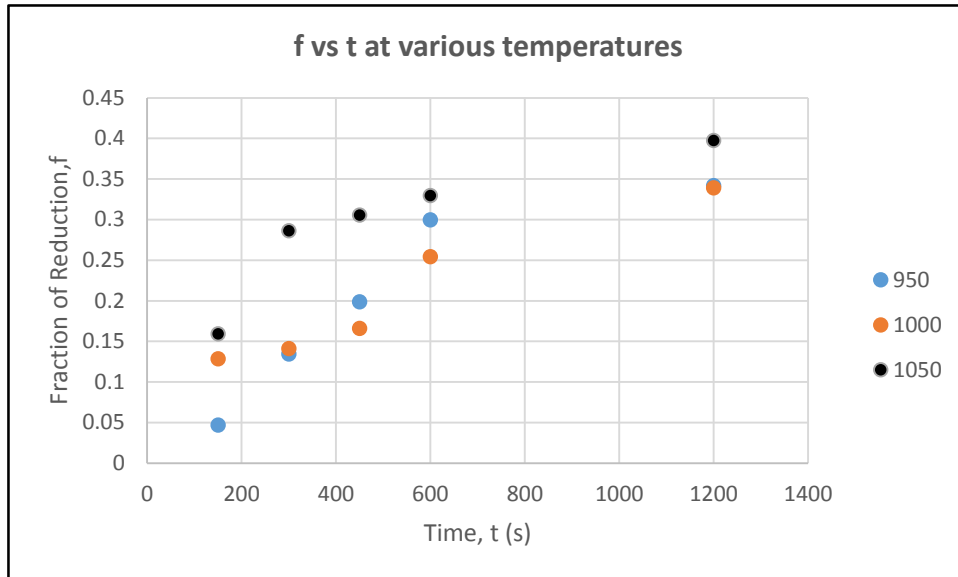


**Fig. 4.31: Reduction curves at various temperature for VIZAG Sludge**

**Table 4.31: Rate of reduction for VIZAG Sludge composite pellet at various temperature**

Sr.no.	Temp (°C)	Temp (K)	(1/T) x 10 <sup>4</sup>	Rate, k X 10 <sup>4</sup>	ln k
1	950	1223	8.18	4.29	-7.75
2	1000	1273	7.86	3.78	-7.88
3	1050	1323	7.56	6.79	-7.30

ln k vs 1/T is plotted (Figure 4.32) for VIZAG Sludge and the slope of the line is found out to calculate activation energy. The activation energy for VIZAG Sludge is found to be 59.28 KJ/mol.

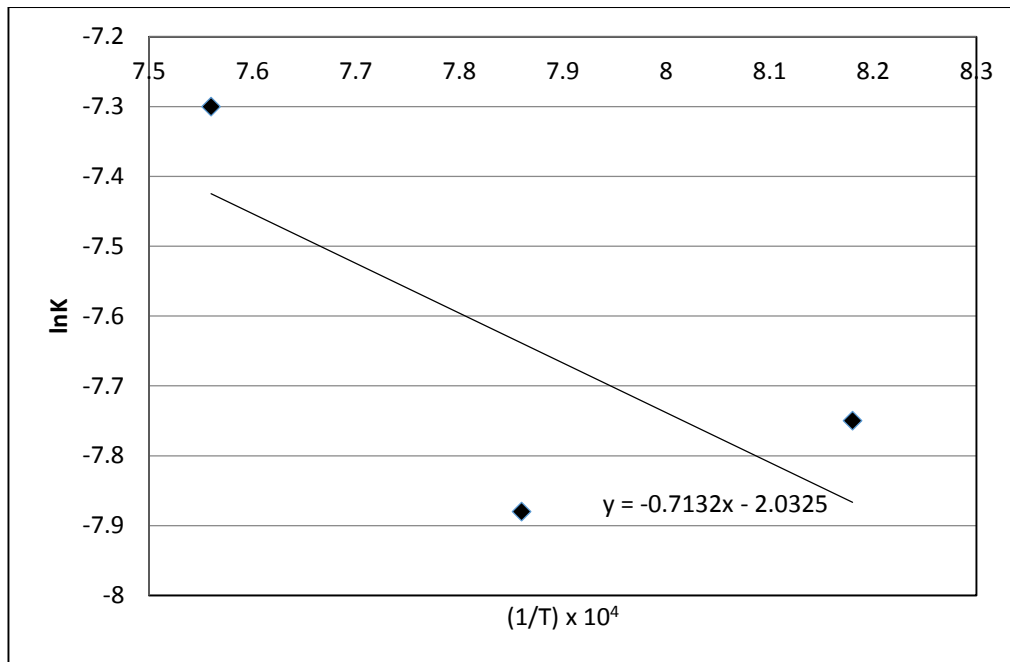


**Fig.4.32:Arrhenius plot for VIZAG Sludge**

**Table 4.32 Values of Activation Energies for All the Composite Pellets**

Sr.No.	Steel Plant Waste	Activation Energy, KJ/mol
1.	JSW Dust	- 52.59
2.	JSW Sludge	- 49.80
3.	VIZAG Sludge	- 59.28

The computed values of activation energies (Table 4.32) are found to be low (49.8 to 59.28 kJ mol<sup>-1</sup>) which means, volatile gases (in particular H<sub>2</sub>) diffuse through porous solid iron oxide particles boundary. Overall reduction is controlled by gasification reactions [C (s) + CO<sub>2</sub> (g) = 2CO (g) and C (s) + H<sub>2</sub>O (g) = CO (g) + H<sub>2</sub> (g)]. In all cases, lower activation energies obtained may be due to the catalytic effect of freshly reduced iron and gangue present in waste, influence the gasification rate.

These above values are comparable to the values of activation energies reported in the literatures. Wang et al. [118] obtained activation energy 68.95 kJ mol<sup>-1</sup> for iron ore-hard coal (low volatile content) pellet. Goswami et al. [119] obtained activation energy 60.75 kJ mol<sup>-1</sup> for fluxed composite pellets. They observed a mixed kinetic model where reduction is initially diffusion controlled and later on chemical reaction controlled. For nonisothermal reduction studies of composite pellets, it was reported [120] that when temperature is lower than 1,073

K (800<sup>0</sup>C) , the reaction is controlled by interface chemical reaction; when the temperature is higher than 1,173 K (900<sup>0</sup>C), the reaction is controlled by diffusion ( $E = 57.3 \text{ kJ mol}^{-1}$ ).

#### 4.7 XRD and SEM

XRD were carried out on reduced composite pellets to identify the phases present in reduced composite pellets with Cu K $\alpha$  (1.56  $\text{A}^0$  ). Figure 4.33 shows XRD peaks for JSW Dust. The result shows the presence of sharp peaks of different phases. The XRD peaks confirm the topochemical pattern of reduction (i.e.  $\text{Fe}_2\text{O}_3 \rightarrow \text{Fe}_3\text{O}_4 \rightarrow \text{FeO} \rightarrow \text{Fe}$ ) occurred in the composite pellets (Table 4.33).

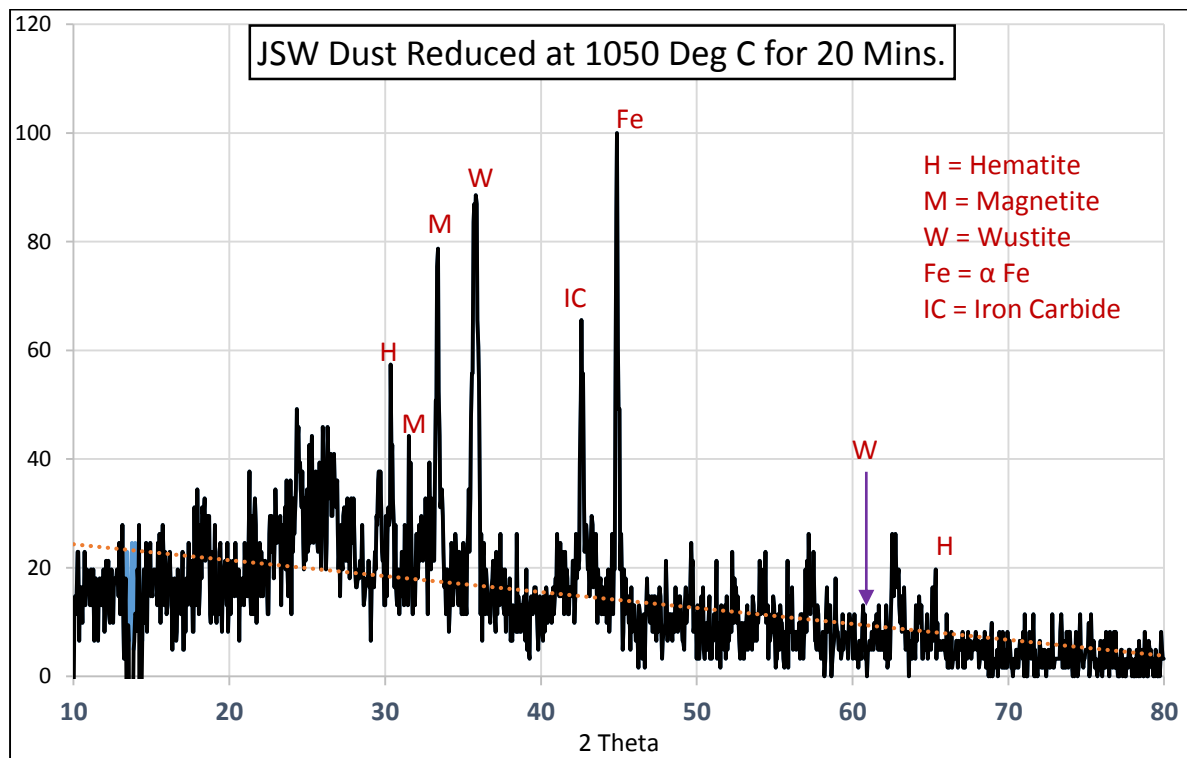


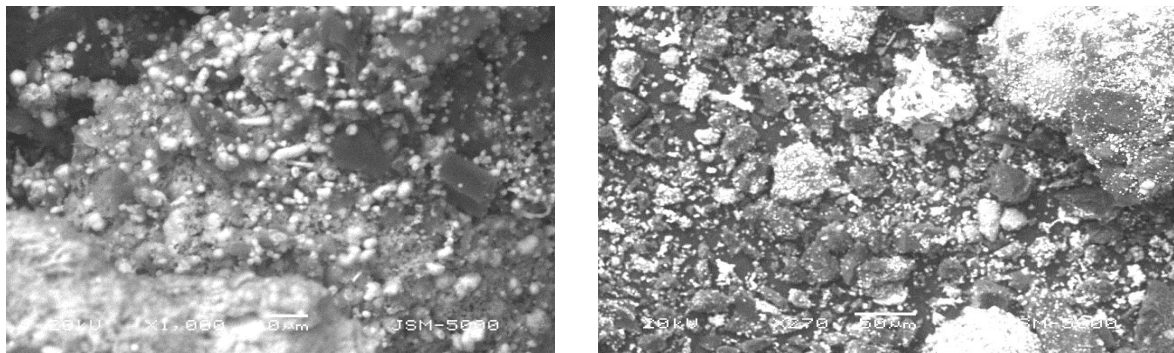
Fig. 4.33: XRD of reduced JSW Dust composite at 1050<sup>0</sup>C for 1200 s

Table 4.33: XRD analysis of reduced JSW Dust composite at 1050<sup>0</sup>C for 1200 s

Sr.No.	d Value Observed	Relative Intensity Observed	d Value Theoretical	Relative Intensity Theoretical	Phases Present
1	2.122	39.34	2.12	40	$\text{Fe}_7\text{C}_3$
2.	2.02	100	2.02	100	$\alpha\text{Fe}$
3.	1.989	16.39	1.989	16	$\text{Fe}_7\text{C}_3$
4	2.96	31.14	2.96	30	$\text{Fe}_3\text{O}_4$

5	2.4245	6.2	2.4243	8	Fe <sub>3</sub> O <sub>4</sub>
6	2.10	19.6	2.099	20	Fe <sub>3</sub> O <sub>4</sub>
7	3.666	34.4	3.686	33	Fe <sub>2</sub> O <sub>3</sub>
8	2.51	83.6	2.49	80	FeO
9	2.50	65.57	2.52	70	FeO
10	1.482	19.67	1.487	22	FeO

Reduced composite pellets were examined by SEM to observe the microstructure. The SEM micrographs (Figure 4.34) confirmed the presence of reduced metallic Fe in reduced composite pellet samples. Fine metallic particles (without sinter) were confirmed the homogeneous reduction mechanism. But the topochemical pattern of reduction in the composite pellets were not found in micrographs.



(a)

(b)

**Fig. 4.34: SEM micrographs of reduced (a) JSW Dust and (b) VIZAG Sludge composite samples at 1050°C for 1200 s(5000X)**

#### 4.8 Conclusion

1. To select the proper binder for pellets preparation, cylindrical shaped briquettes were prepared and tested. Different binders like lime, slaked lime, bentonite, molasses etc. and their combination were used to prepare briquettes and their properties (compressive strength, drop strength and shatter index) were evaluated.
2. It was found that TB3 (with 7.5 pct fly ash, 5 pct lime and 5 pct molasses) gave good green drop strength (8) and dry drop strength (24), but TB6 (with 7.5 pct fly ash, 5 pct slake lime and 5 pct molasses) gave higher compressive strength (107.8 N/briquette)

and as well as good shatter strength (7.17); that means slake lime was more effective to form calcite due to CO<sub>2</sub> passing.

3. Further trails were done with starch and molasses as binder separately with JSW dust and Taguchi technique was used, for selection of binder proportion in combination for pellets production. It was found that E2 (with 2.5 pct starch and 5 pct molasses) gave highest strength (1196.82 N/briquette) and lower shatter index (0.18).
4. Binders were selected for pellet making based on briquettes formation and proper strength of briquettes. Waste-coal composite pellets were prepared with binder combination as: i) for JSW Dust: 7.5 pct starch and 5.0 pct molasses, ii) for JSW Sludge: 5.0 pct starch and 2.5 pct molasses, and iii) for VIZAG Sludge: 7.5 pct starch and 2.5 pct molasses.
5. The reducibility studies were done with variation of temperature (950, 1000 and 1050<sup>0</sup>C) and time (150, 300, 450, 600 and 1200 s).
6. It was found that fraction of reduction increases with increasing in temperature and time for all three materials.
7. The activation energies were - 52.59, - 49.80 and - 59.28 KJ/mol for JSW Dust, JSW Sludge and VIZAG Sludge composites respectively.
8. The activation energies for composite pellets reduction are found to be low (49.8–59.28 kJ mol<sup>-1</sup>) which means, volatile gases (in particular H<sub>2</sub>) diffused through porous solid iron oxide particles boundary. Overall reduction was controlled by gasification reactions.
9. From XRD, it is confirmed that the reduction take place in topochemical manner, i.e. stage wise reduction.
10. It is also confirmed that the presence of metallic iron in reduced composite by SEM.